J Neurophysiol 123: 367–391, 2020.
First published November 20, 2019; doi:10.1152/jn.00432.2019.

RESEARCH ARTICLE | *Neural Circuits*

Eye position signals in the dorsal pulvinar during fixation and goal-directed saccades

Lukas Schneider,[1,2] Adan-Ulises Dominguez-Vargas,[1,3] Lydia Gibson,[1,2] Igor Kagan,[1,2,4]* and Melanie Wilke[1,2,4]*

[1]*Decision and Awareness Group, Cognitive Neuroscience Laboratory, German Primate Center, Leibniz Institute for Primate Research, Goettingen, Germany;* [2]*Department of Cognitive Neurology, University of Goettingen, Goettingen, Germany;* [3]*Escuela Nacional de Estudios Superiores Unidad-León, Universidad Nacional Autónoma de México, León, Guanajuato, Mexico; and* [4]*Leibniz ScienceCampus Primate Cognition, Goettingen, Germany*

Submitted 9 July 2019; accepted in final form 18 November 2019

Schneider L, Dominguez-Vargas AU, Gibson L, Kagan I, Wilke M. Eye position signals in the dorsal pulvinar during fixation and goal-directed saccades. *J Neurophysiol* 123: 367–391, 2020. First published November 20, 2019; doi:10.1152/jn.00432.2019.—Sensorimotor cortical areas contain eye position information thought to ensure perceptual stability across saccades and underlie spatial transformations supporting goal-directed actions. One pathway by which eye position signals could be relayed to and across cortical areas is via the dorsal pulvinar. Several studies have demonstrated saccade-related activity in the dorsal pulvinar, and we have recently shown that many neurons exhibit postsaccadic spatial preference. In addition, dorsal pulvinar lesions lead to gaze-holding deficits expressed as nystagmus or ipsilesional gaze bias, prompting us to investigate the effects of eye position. We tested three starting eye positions (−15°, 0°, 15°) in monkeys performing a visually cued memory saccade task. We found two main types of gaze dependence. First, ~50% of neurons showed dependence on static gaze direction during initial and postsaccadic fixation, and might be signaling the position of the eyes in the orbit or coding foveal targets in a head/body/world-centered reference frame. The population-derived eye position signal lagged behind the saccade. Second, many neurons showed a combination of eye-centered and gaze-dependent modulation of visual, memory, and saccadic responses to a peripheral target. A small subset showed effects consistent with eye position-dependent gain modulation. Analysis of reference frames across task epochs from visual cue to postsaccadic fixation indicated a transition from predominantly eye-centered encoding to representation of final gaze or foveated locations in nonretinocentric coordinates. These results show that dorsal pulvinar neurons carry information about eye position, which could contribute to steady gaze during postural changes and to reference frame transformations for visually guided eye and limb movements.

NEW & NOTEWORTHY Work on the pulvinar focused on eye-centered visuospatial representations, but position of the eyes in the orbit is also an important factor that needs to be taken into account during spatial orienting and goal-directed reaching. We show that dorsal pulvinar neurons are influenced by eye position. Gaze direction modulated ongoing firing during stable fixation, as well as visual and saccade responses to peripheral targets, suggesting involvement of the dorsal pulvinar in spatial coordinate transformations.

eye movements; macaque; memory saccades; orbital gaze position; reference frames

INTRODUCTION

Information about eye position is ubiquitous in the primate brain and is critical for visually guided behavior. Neurons modulated by the position of the eyes in the orbit have been reported in brain stem nuclei (Hernández et al. 2019; Luschei and Fuchs 1972), superior colliculus (SC) (Campos et al. 2006; Van Opstal et al. 1995), inferior colliculus (Porter et al. 2006), thalamus (Schlag-Rey and Schlag 1984; Tanaka 2007; Wyder et al. 2003), cerebellum (Noda and Warabi 1982), and numerous cortical regions including visual and frontoparietal cortices (Andersen et al. 1990; Bizzi 1968; Morris et al. 2013; Squatrito and Maioli 1996; Trotter and Celebrini 1999; Wang et al. 2007). These eye position signals might subserve different functions. In the visual/oculomotor domain, eye position signals could enable stable vision, the discrimination between self- and external motion, precise stimulus localization across eye movements, and postsaccadic updating (Sommer and Wurtz 2008; Wurtz et al. 2011a). During intersaccadic periods, these signals might enable stable fixation, including vergence of the eyes and smooth pursuit (Squatrito and Maioli 1996). In the context of visually guided limb and body movements, eye position signals might serve to transform the retinal location of visual stimuli into head-, limb- or trunk-centered reference frames (Andersen et al. 1993; Colby 1998; Pouget and Snyder 2000). In most experimental situations, the head is immobilized, and thus the position of eyes in the orbit is equivalent to gaze direction, or angle.

Taking the current gaze angle into account is also important for the visual guidance of movements since visual inputs enter the brain in eye-centered (retinocentric) coordinates, but control of limb movements requires locating the objects in respect to the body and the world. A common model of how the brain deals with those spatial reference frame transformations are the so called "gain fields," manifested as a modulation of sensory-evoked, motor preparation, or movement-evoked responses by the current eye position on a single-neuron level such that the

* I. Kagan and M. Wilke shared senior authorship; senior authors are listed alphabetically.

Address for reprint requests and other correspondence: I. Kagan, German Primate Center, Leibniz Institute for Primate Research, Kellnerweg 4, Goettingen 37077, Germany (e-mail: ikagan@dpz.eu).

  ISSN 0022-3077.

neural population response simultaneously represents the retinal and body-centered stimulus location (Andersen et al. 1990; Cohen and Andersen 2002; Pouget and Snyder 2000; Salinas and Abbott 2001). Neurons that exhibit a modulation of visual responses by eye position were first reported in the intralaminar nuclei of the thalamus (Schlag et al. 1980) and the superior colliculus (SC) in cats (Peck et al. 1980), and later in monkeys in the ventral (retinotopically organized) pulvinar (Robinson et al. 1990). A systematic assessment of spatial tuning at different eye positions revealed gain field properties across numerous cortical regions, including parietal areas [e.g., lateral intraparietal area (LIP), ventral intraparietal area (VIP), medial intraparietal area (MIP), area 7a], the frontal eye fields (FEF), posterior cingulate, and middle superior temporal area (MST) (Andersen et al. 1990; Bremmer et al. 1999, 2002; Caruso et al. 2018; Dean and Platt 2006; Galletti et al. 1995; Lehky et al. 2016; Squatrito and Maioli 1996).

It is not entirely clear how this eye position information is distributed across cortical areas. A region that could possibly fulfill this function is the dorsal pulvinar (dPul) (Arcaro et al. 2018; Sherman and Guillery 2002). The dorsal pulvinar, consisting of the medial pulvinar and dorsal part of the lateral pulvinar, is in a good anatomical and functional position to transfer gaze-related information to and across frontoparietal and superior temporal cortices (Bridge et al. 2016; Grieve et al. 2000; Halassa and Kastner 2017; Wurtz et al. 2011a). The dorsal pulvinar receives direct input from the intermediate and deep layers of the superior colliculus (Baldwin and Bourne 2017; Benevento and Standage 1983) and is reciprocally interconnected with prefrontal [FEF, dorsal lateral prefrontal cortex (dlPFC)], dorsal premotor (PMd), posterior parietal (LIP, MIP, VIP, area 7), and superior temporal sulcus regions such as MST and temporal parietal occipital area (TPO) (Cappe et al. 2012; Gutierrez et al. 2000; Kaas and Lyon 2007; Romanski et al. 1997; Yeterian and Pandya 1989). Beyond its anatomical connections, electrophysiological and lesion studies suggest a critical role of the dorsal pulvinar in spatial attention (Fiebelkorn et al. 2019; Petersen et al. 1987) and oculomotor behavior. Specifically, response properties of dorsal pulvinar neurons in monkeys partially resemble those of its diverse cortical projection targets, such as parietal cortex (e.g., enhancement for visual stimuli that indicate an upcoming saccade target) (Robinson 1993). Although the dorsal pulvinar is not retinotopically organized and its neurons have large receptive fields, they discharge in the context of saccade tasks in visual cue and saccade execution phases, exhibiting an overall preference for contralateral visual cue, perisaccadic, and postsaccadic responses (Benevento and Port 1995; Dominguez-Vargas et al. 2017; Petersen et al. 1985).

In line with its neuronal properties, unilateral pharmacological inactivation of the dorsal pulvinar in macaques results in a decreased ability to shift attention into the contralesional field (Robinson and Petersen 1992) and a saccade choice bias toward the ipsilesional field (Wilke et al. 2010, 2013). Human patient studies are largely consistent with those results, showing contralesional spatial deficits (Arend et al. 2008; Karnath et al. 2002; Van der Stigchel et al. 2010). Apart from eye movement selection, the dorsal pulvinar also plays a critical role in other visuomotor behaviors such as reaching and grasping: its neural activity correlates with reach movements (Acuña et al. 1990; Cudeiro et al. 1989), and inactivation/lesions in monkeys and humans lead to hand- and space-specific deficits in reach-and-grasp tasks (Wilke et al. 2010, 2018).

Based on those anatomical and functional results, it has been proposed that the dorsal pulvinar is involved in reference frame transformations critical for eye-hand behavior, although this has not been directly demonstrated (Bridge et al. 2016; Grieve et al. 2000). In fact, very basic questions, such as whether dorsal pulvinar neurons carry eye position signals and how those interact with visual cue responses, have not been addressed. Even the effect of static eye position on ongoing firing has not been tested, although the presence of tonic firing during initial and postsaccadic fixation (Dominguez-Vargas et al. 2017) as well as nystagmus and smooth pursuit deficits following dorsal pulvinar inactivation/lesions suggest that it might be also involved in gaze stabilization (Ohtsuka et al. 1991; Wilke et al. 2010, 2018).

In the current study we investigated the effect of eye position on initial fixation, visual, memory, saccade, and postsaccadic responses in monkeys performing a memory-guided saccade task. We demonstrate that about half of dorsal pulvinar cells are modulated by steady gaze position before visual cue onset and long after the saccade. We also demonstrate a gaze-dependent modulation of visual and saccadic activity, providing a possible substrate for head- or body-centered spatial representations.

MATERIALS AND METHODS

All experimental procedures were conducted in accordance with the European Directive 2010/63/EU, the corresponding German law governing animal welfare, and German Primate Center institutional guidelines. The procedures were approved by the responsible government agency (LAVES, Oldenburg, Germany).

Animal Preparation

Two adult male rhesus monkeys (*Macaca mulatta*), *monkey C* and *monkey L*, weighing 8 and 9 kg, respectively, were used. In an initial surgery, monkeys were implanted with a magnetic resonance imaging (MRI) compatible polyetheretherketone (PEEK) headpost embedded in a bone cement headcap (Palacos with gentamicin; BioMet) anchored by ceramic screws (Rogue Research, Canada) under general anesthesia and aseptic conditions. MR-visible markers were embedded in the headcap to aid the planning of the chamber in stereotaxic space with the MR-guided stereotaxic navigation software Planner (https://github.com/shayo/Planner) (Ohayon and Tsao 2012). A separate surgery was performed to implant a PEEK MRI-compatible chamber(s) (inside diameter 22 mm) allowing access to the pulvinar [*monkey C*, right hemisphere: center at 0.5A/14.5R mm, tilted −11P/27R degrees; *monkey L*, right hemisphere: center at −3.12P/20.2R mm, tilted −18P/37R degrees; *monkey L*, left hemisphere: center at −3P/20L, tilted −18P/-38L; the coordinates are relative to stereotaxic zero (A, anterior; P, posterior; L, left; R, right); the tilts are relative to the vertical axis normal to stereotaxic plane (P, posterior, top of the chamber tilted toward the back of the head; L/R, left/right, top of the chamber tilted toward the corresponding ear)]. After chamber positioning was confirmed with a postsurgical MRI, a partial craniotomy was made inside the chamber. The exposed dura was covered with a silicone elastomer (Kwik-sil, World Precision Instruments) to reduce the granulation tissue growth and dura thickening.

MR Imaging

Monkeys were scanned in a 3T MRI scanner (Siemens Magnetom TIM Trio). Full-head T1-weighted scans (3-dimensional magnetiza-

tion-prepared rapid gradient-echo, 0.5 mm isometric) were acquired before and after chamber implantation, in awake (*monkey C*) or anesthetized state (*monkey L*), using either built-in gradient body transmit coil and a custom single-loop receive coil or a custom single-loop transmit and four-channel receive coil (Windmiller Kolster Scientific).

In addition to pre- and postimplantation scans, similar T1-weighted scans as well as T2-weighted scans (rapid acquisition with relaxation enhancement, RARE; 0.25 mm in-plane resolution, 1-mm slice thickness) were periodically acquired during the course of experiments, in either awake (*monkey C*) or sedated state (*monkey L*), to confirm electrode positioning. These images were acquired with the chamber and a custom-made MR-compatible polyetherimide (Ultem) grid (0.8-mm hole spacing, 0.45-mm hole diameter) filled with gadolinium (Magnevist, Bayer, Germany)-saline solution (proportion 1:200), with tungsten rods inserted in predefined grid locations for alignment purposes. The electrode penetration trajectory and the recording depth were visualized using platinum-iridium electrodes [FHC; 100-mm-length platinum-iridium 125-μm-thick core, initial 2 cm glass coated, total thickness of 230 μm including polyamide tubing coating, UEPLEFSS (UEIK1; FHC)], advanced by an MRI-compatible custom-made plastic XYZ manipulator drive through the corresponding grid hole. For the dura penetration, the electrode was protected by a custom-made MRI-compatible fused silica guide tube (320-μm inner diameter, 430-μm outer diameter; Polymicro Technologies). A stopper (530-μm inner diameter, 665-μm outer diameter, 23-gauge MicroFil; World Precision Instruments) ensured that the guide tube only penetrated the dura and minimally the cortex below. Prior to penetration, the electrode tip was aligned to the guide tube tip and was held in place by a drop of melted Vaseline. The guide tube was filled with sterile silicone oil before electrode insertion, to ensure smooth electrode travel and to prevent the backflow of cerebrospinal fluid. T1- and T2-weighted scans were coregistered and transformed into "chamber normal" (aligned to the chamber vertical axis) and to anterior commissure-posterior commissure (AC-PC) space for electrode targeting and visualization in BrainVoyagerQX (Brain Innovation, The Netherlands) and Planner (Ohayon and Tsao 2012).

Gaze Modulation Task

Monkeys sat in a dark room in custom-made primate chairs with their heads restrained 30 cm away from a 27-in. LED display (60-Hz refresh rate, model HN274H; Acer Inc.) covering a range of 84 × 53 visual degrees for *monkey C* and 91 × 59 for *monkey L*. The gaze position of the right eye was monitored at 220 Hz using an MCU02 ViewPoint infrared EyeTracker (Arrington Research Inc.). Eye position was calibrated using linear gains and offsets for horizontal and vertical axes, during visually guided saccades, and recalibrated using MATLAB (The MathWorks, Inc.) geometric transformation function fitgeotrans.m with second-degree polynomial fit. All stimulus presentation and behavioral control tasks were programmed in MATLAB and the Psychophysics Toolbox (Brainard 1997).

The structure of the task is shown in Fig. 1*A*. A trial started with the onset of the fixation point of 1° diameter either at the center or 15° left or right to the center of the screen. After the monkey acquired and held fixation within a 5° radius for 500 ms, a peripheral cue (also 1° diameter) was displayed for 300 ms signaling the upcoming saccade target location. For each trial, one of eight cue/target locations was used. These eight positions were arranged in a virtual rectangle around the initial fixation point, at 0°, 15°, or −15° horizontally and 0°, 10°, or −10° vertically, resulting in 24 different spatial conditions (8 target locations for each of the 3 initial fixation positions). Monkeys were required to maintain fixation throughout the cue period and also throughout the subsequent memory period (1,000 ms), after which the central fixation point disappeared, allowing monkeys to saccade to the instructed target location. This time point will be referred to as the "Go signal." After a saccade and fixation inside a 5° radius window surrounding the remembered target location for 200 ms, the target became visible. After an additional 500 ms of peripheral fixation, the trial was completed and the monkey obtained a liquid reward after a delay of 200 ms. The intertrial interval for successful and unsuccessful trials was 2,500 ms. All initial fixation positions (3) and retinocentric target locations (8) were pseudorandomized.

Electrophysiological Recordings

Dorsal pulvinar neuronal activity was recorded with up to four individually movable single platinum-tungsten (95–5%) quartz glass-insulated electrodes with impedance ranging from 1 to 2 MΩ for *monkey C* and from 1.3 to 1.8 MΩ for *monkey L*, using a chamber-mounted five-channel Mini Matrix microdrive (Thomas Recording, Germany). Single custom-made stainless steel guide tubes (27 gauge), made from Spinocan spinal needles (B. Braun Melsungen AG, Germany) filled with silicone oil (Thomas Recording), with a metal funnel attached to the microdrive nozzle were used to protect electrodes during grid insertion and dura penetration. A reference tungsten rod or a silver wire was placed in the chamber filled with saline and was connected to the chassis of the drive. Neuronal signals were amplified (×20 head stage, Thomas Recording; ×5, 128- or 32-channel PZ2 preamplifier, Tucker-Davis Technologies), digitized at 24 kHz and 16-bit resolution, and sent via fiber optics to an RZ2 BioAmp processor (Tucker-Davis Technologies) for online filtering (300–5,000 Hz bandpass), display, and storage on a hard drive together with behavioral and timing data streams.

Data Analysis

Saccade definition. Instantaneous saccade velocity was calculated sample by sample as the square root of the sum of squared interpolated (220 Hz to 1 kHz) and smoothed (12-ms moving average rectangular window) horizontal and vertical eye position traces, and then smoothed again (12-ms moving average rectangular window). Saccade onset was defined as the first eye position change after the go signal that exceeded a velocity threshold of 200°/s; saccade end was defined as the first eye position change below 50°/s after saccade onset. Average saccade latency across sessions was 192 ± 3 ms (202 ± 2 ms for *monkey C*, 184 ± 2 ms for *monkey L*), average saccade duration 45 ± 0.2 ms (44.9 ± 0.3 and 45 ± 0.3 ms), and average maximum saccade velocity was 562 ± 7°/s (529 ± 5 and 589 ± 4°/s). Supplemental Tables S1 and S2 (all Supplemental Material is available at https://doi.org/10.6084/m9.figshare.10055318.v1) show saccade amplitude and the velocity per initial gaze and target eccentricity. For corrective saccades (small refixation saccades after target reappearance), 20°/s and 10°/s were used as onset and offset velocity thresholds. Corrective saccades were common in both monkeys (81 ± 2% and 96 ± 1% of all trials), with an average latency of 136 ± 4 ms (151 ± 4 and 124 ± 2 ms) after target reappearance and average amplitude of 1.4 ± 0.1° (0.9 ± 0.03° and 1.7 ± 0.05°). Final gaze positions are shown in Supplemental Table S3. All values in *Data Analysis* are session means ± SE, with values in parentheses for *monkey C* and for *monkey L* given separately. For visualization of saccade end points and final gaze positions, as a function of the initial gaze, see Supplemental Fig. S1.

Data set and unit selection criteria. All recorded voltage drops that surpassed an online visually determined threshold were defined as potential spikes. Spike sorting was done in Offline Sorter v.3.3.5 (Plexon), using a waveform template algorithm, after templates were defined by manual clustering in principle component space using the first three principle components, as well as the recording time axis. Based on inspection of spike shapes, cluster shapes, and interspike intervals, clusters were categorized as single units, multiunits, or rejected "noise."

In total, 325 single and multiunits were recorded in the dorsal pulvinar in 22 sessions where monkeys performed the gaze modula-

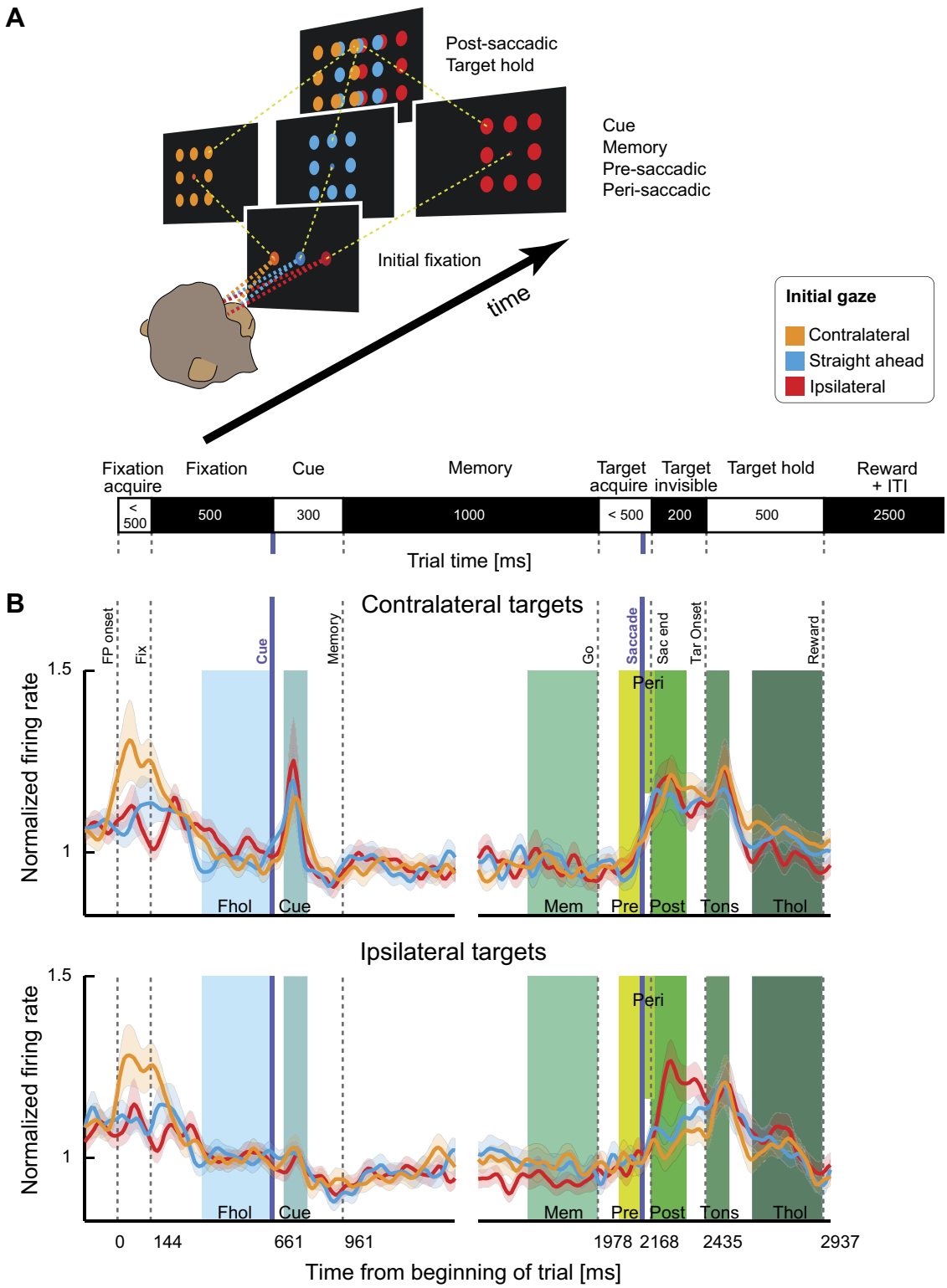

Fig. 1. Task and population average. *A*: task conditions. A trial started at 1 of 3 initial fixation positions (Fixation). One of 8 target positions surrounding the fixation point was flashed (Cue). Monkeys had to remember the location while keeping fixation (Memory) until the fixation point disappeared, prompting a saccade to the target (Target acquire). After the monkey held fixation for a short period (Target invisible), the target reappeared as a confirmation (Target hold). *B*: normalized population peristimulus time histograms and standard errors across units for each initial gaze position for contralateral and ipsilateral targets (relative to initial gaze position). Vertical lines indicate average onset of events across all trials: fixation point onset (FP onset), the monkey acquiring fixation (Fix), the cue onset (Cue), the cue offset and beginning of the memory period (Memory), the offset of the central fixation point (Go), the saccade onset (Saccade), the monkey acquiring the invisible target location (Sac end), the onset of the confirmation target (Tar Onset), and the end of the trial (Reward). Discontinuous traces indicate 2 different alignments to cue onset and saccade onset (purple lines). Colored boxes mark analysis epochs: fixation hold (Fhol), cue onset (Cue), memory (Mem), presaccadic (Pre), perisaccadic (Peri), postsaccadic (Post), target onset (Tons), and target hold (Thol) (see MATERIALS AND METHODS). ITI, intertrial interval.

tion task (*monkey C*: right hemisphere, 134; *monkey L*: left hemisphere, 191). Of these, 275 units (93 *monkey C*, 182 *monkey L*) fulfilled initial analysis selection criteria (stable discriminability across time and reasonable signal-to-noise ratio, assessed by inspection). Of these 275 units, 268 units (86 *monkey C*, 182 *monkey L*) were recorded for at least four successful trials for each of the initial gaze positions. These 268 units were used for initial gaze analysis. Of these 268 units, 238 units (60 *monkey C*, 178 *monkey L*, collected in 20 sessions) were recorded for at least four successful trials for each combination of initial gaze and retinocentric target location (24 conditions). The median (across units) of the minimal number of trials per condition was nine trials (with a range from 4 to 19 trials). Most units (209 of 238) were recorded for at least eight trials per condition. The median (across units) of the average number of trials per condition was 9.8 with a range from 5 to 20.

These 238 units were used for further gaze-dependent analysis. Of these 238 units, 172 units were categorized as well-isolated stable single units. The distribution of average firing rates for single units and multiunits across the entire trial duration is shown in Supplemental Fig. S2. Besides Supplemental Fig. S9, which reproduces several analyses using only single units, all analyses were performed on single and multiunits together.

Epoch definitions and modulation. For each trial, and each epoch of interest, firing rates were computed by counting spikes within the epoch and dividing by the epoch duration. The following epochs were analyzed: fixation hold (last 300 ms of central fixation), cue onset (50 to 150 ms after cue onset), memory (last 300 ms of the memory period), presaccadic (100 to 10 ms before saccade onset), perisaccadic (10 ms before to 50 ms after saccade onset), postsaccadic (first 150 ms after the invisible peripheral target was acquired), target onset (20 to 120 ms after the target became visible), and target hold (last 300 ms of fixation of the peripheral target).

For analysis of basic response types in the entire population (Supplemental Fig. S3), trials were grouped by either retinocentric or screen-centered target location. We performed two ANOVAs on firing rates of each unit in each epoch: a two-way ANOVA with factors initial gaze position and retinocentric target location and a one-way ANOVA dependent on screen-centered target location. In addition, we computed retinocentric hemifield preferences for all units that showed a main effect of retinocentric target location in the respective epoch and screen-centered hemifield preferences for all units that showed an effect of screen-centered target location. To this end, data from all contralateral and ipsilateral hemifield targets were combined. Hemifield tuning in each epoch was determined by unpaired *t* tests comparing firing rates in ipsilateral trials with firing rates in contralateral trials. The hemifield with the higher firing rate was marked, if there was a significant difference.

Enhancement or suppression of neuronal activity in each epoch was defined by significant paired *t* tests comparing firing rates to a respective preceding baseline epoch, across all trials. For the fixation hold epoch, intertrial interval served as baseline, whereas for cue onset and memory epochs, the fixation hold epoch served as baseline. The memory epoch served as baseline for all subsequent epochs.

Peristimulus time histograms. Spike density functions were computed at a bin size of 10 ms using a Gaussian kernel ($\sigma = 20$ ms). Example peristimulus time histograms (PSTHs) show spike densities averaged across all trials with the same initial fixation position. For population PSTHs, we first normalized spike density functions for each unit by dividing by the average firing rate in the fixation hold epoch (across all trials) and then computed average spike density and standard error (across units) for each initial gaze position and contralateral/ipsilateral retinocentric target positions individually.

Gaze position-dependent analysis. To evaluate effects of gaze position on neuronal activity of each unit, we analyzed initial and final gaze position effects. An effect of initial gaze position was determined by a one-way ANOVA on firing rates during the fixation hold epoch with 3 initial gaze positions as the independent factor, and an effect of final gaze position was determined by a one-way ANOVA on firing rates during the target hold epoch with 15 final gaze positions as the independent factor. To dissociate horizontal and vertical gaze tuning, an additional two-way ANOVA was performed with the factors horizontal and vertical final gaze position.

To evaluate if gaze dependence varied systematically with horizontal and/or vertical gaze position, units with a main effect along the respective dimension were further grouped by monotonic and nonmonotonic gaze-dependent activity. Monotonic gaze dependence was defined by *1*) a significant difference between firing rates for the most peripheral positions (unpaired *t* test) and *2*) no significant opposite sign differences in firing rates between any two neighboring positions. All other units that showed an effect in the ANOVA were classified as nonmonotonic. Units showing nonmonotonic initial gaze preference were further grouped into central preference (highest activity for straight-ahead gaze) and peripheral preference (lowest activity for straight-ahead gaze). For better visualization, firing rates for each unit were normalized by dividing average responses for each of the three initial/final gaze positions by the maximum average firing rate across all positions.

To utilize the 5×3 two-dimensional (2D) distribution of target hold targets, three different models were used to fit final gaze dependent firing rates in a 2D plane: a linear model, a sigmoidal model (assuming saturation effects) and a Gaussian model (assuming nonmonotonic gaze dependence consistent with a peak or a trough). For each of the 15 final gaze positions, we derived the mean and variance of firing rates. Mean firing rates were used as the dependent variables, and the inverse of the variances as weights. This analysis was only performed on units that showed a main effect of final gaze position, using a one-way ANOVA ($n = 156$). Fitting parameters were determined using an iterative nonlinear least-squares method (400 iterations). The best fit (highest adjusted R^2) was reported if at least one of the models explained firing rate variation in the 15 final gaze positions significantly better ($P < 0.05$, stepwisefit.m, MATLAB) than a uniform firing rate.

In the linear model, three fitting parameters for each unit were determined: *1*) a uniform baseline firing rate, *2*) a linear slope, and *3*) the direction of firing rate increase. The baseline was bounded by the minimum and maximum firing rate, whereas the other two parameters were unbounded.

In the sigmoidal model, we used a logistic function to fit firing rates. Six fitting parameters for each unit were determined: *1*) a uniform baseline firing rate, *2*) the response strength, *3*) the steepness of the logistic function, *4* and *5*) the horizontal and the vertical location of the midpoint, and *6*) the direction of firing rate increase. Importantly, the midpoint was always kept within the dimensions of the target array ($-17.5°$ to $17.5°$ horizontally and $-5°$ to $5°$ vertically). The response strength was bounded between 0% and 200% of the difference between the maximal and the minimal firing rate, the steepness was kept between 0 and 0.3 (so that the linear part of the sigmoidal would cover at least one target position), and the baseline was bounded by the minimum and maximum firing rate.

In the Gaussian model, seven fitting parameters were determined for each unit, allowing an elliptic Gaussian distribution with peak (or trough) at the center. The fitting parameters were *1*) a uniform baseline firing rate, *2*) the response strength in the center of zone, *3*) horizontal and *4*) vertical location of the center of the response zone, *5* and *6*) two standard deviations describing semi-minor and semi-major axes, and *7*) an angle of rotation of these axes. Importantly, the response zone center was always kept within the dimensions of the target array ($-17.5°$ to $17.5°$ horizontally and $-5°$ to $5°$ vertically). The response strength was bounded by -150% and 150% of the original maximum response strength, standard deviations were bounded by $1.5°$ and $12°$ (with a minimum ratio of standard deviation in both directions of 1:4), and the baseline by the minimum and maximum firing rate.

To investigate the timing of gaze dependent effects, we performed an analysis similar to that of Morris et al. (2012). In short, we derived population activity separately for neurons that shifted from a low to a high firing rate (POS), and for units that shifted from a high to a low firing rate (NEG), across saccades. The hypothetical ongoing eye position signal was obtained by subtracting NEG from POS. For each condition (a unique combination of initial and final gaze, 24 combinations), POS and NEG were derived by taking the median firing rate across all units that showed a significant increase (or decrease, respectively) from the fixation period before the saccade to final fixation period after the saccade in that specific condition. Resulting POS and NEG curves were then averaged across conditions. Responses were normalized per unit to represent percent change from baseline. The baseline was defined as the mean firing rate across the presaccadic and postsaccadic fixation periods, separately for each condition. Given the restrictions of our task timing, instead of varying the fixation periods and averaging across all potential combinations of periods as was done in the original study of Morris et al., we selected two different fixation periods before the saccade, the initial fixation hold (last 300 ms of central fixation before the cue) and memory (last 300 ms of the memory period), and only one postsaccadic period, the target hold period (last 300 ms of fixating the peripheral target).

To test if the spatial preferences of gaze-dependent responses are affected by the task epoch, we compared initial (fixation hold) and final (target hold) gaze contralaterality indices across all units. Contralaterality indices were computed as $(C - I)/(C + I)$, where C and I are the average firing rates for contralateral and ipsilateral gaze positions, relative to the center of the screen. For final gaze contralaterality indices six ipsilateral and six contralateral gaze positions were combined. Straight-ahead gaze positions were not used for this analysis.

Gaze-dependent modulation of spatially contingent task epochs. To evaluate the presence of not purely retinocentric response fields for each unit, average firing rates in each epoch were tested with a two-way ANOVA, using the factors initial gaze position and retinocentric target location.

To evaluate the relationship of gaze and cue tuning across units, we first correlated initial gaze and retinocentric cue spatial preferences and second tested if there was a difference in response modulation by comparing absolute strength of gaze and cue spatial preferences using Wilcoxon's signed rank test. In total, we performed four different comparisons: spatial preferences were taken as either raw firing rate differences ($C - I$, where C and I are the average firing rates in contralateral and ipsilateral trials) or contralaterality indices ($(C - I)/(C + I)$, and gaze preference was derived from either fixation hold (Fhol) or cue onset (Cue) epoch. Spatial cue preference was computed using all three gaze positions, combining all cues contralateral or ipsilateral relative to the current gaze.

Modulation of retinocentric encoding by gaze position. To evaluate the presence of gain fields for each unit and each epoch, we used a model-free approach that does not assume any specific shape of the tuning function. First, we computed confidence intervals for tuning vector length and direction, independently for each initial gaze position, using hierarchical bootstrapping. One thousand bootstrapping iterations were performed for each unit, epoch, and initial gaze position, with 10 trials (with replacement) sampled for each retinocentric target position. Normalized tuning vectors for each sampled trial were computed with direction equal to the direction of the retinocentric target position and the length equal to the firing rate. The average tuning vector for the current bootstrap iteration was then computed as the sum of normalized firing rate vectors across all sampled trials. To evaluate significance of gain and tuning vector shifts, the 95% confidence intervals of differences in amplitude and direction of the bootstrapped tuning vectors for each pair of initial gaze positions were computed, independently for each epoch. Units in which, for at least one of these comparisons between gaze positions, the confidence interval of amplitude or direction differences did not overlap with zero were marked as showing gain field properties or response field shifts, respectively. This analysis was performed only on units that showed a main effect of retinocentric target location in the respective epoch in the two-way ANOVA mentioned before.

To estimate gain effect size, we calculated the percent change in the amplitude of the average bootstrapped tuning vector across three initial gaze positions for each unit as $100 \times (A_{max} - A_{min})/A_{max}$, where A_{max} is the amplitude of the largest and A_{min} the amplitude of the smallest of the three average tuning vectors.

Reference frame estimation. To see if pulvinar responses were better explained by a retinocentric or screen-centered reference frames (i.e., relative to the locations on the screen, which could signify head-, body-, or world-centered representations, since the head was immobilized relative to the screen and the body orientation was not explicitly controlled), we grouped the trials either by retinocentric target location or by the target location on the screen and compared average correlation coefficients (ACCs) in both arrangements for each unit (Mullette-Gillman et al. 2005). For each reference frame, ACCs were computed by correlating responses for two of three initial gaze positions at a time and then averaging the three correlation coefficients. For screen-centered encoding, we used only locations that were available for both initial gaze positions for every correlation pair. To estimate significance, we performed 1,000 bootstrap iterations using 80% of the trials for each location at a time. This allowed us to derive 95% confidence intervals for both retinocentric and screen-centered ACCs. Significant encoding in the respective reference frame was reported if *1*) the confidence interval was above zero, *2*) the confidence interval for this reference frame was above the ACC for the other reference frame, and *3*) the ACC for this reference frame was above the confidence interval for the other reference frame. In other words, both confidence intervals should be above or below the unity line diagonal.

RESULTS

We recorded single- and multiunit activity in two monkeys performing a memory-guided saccade task with variation of initial gaze (fixation) position (Fig. 1*A*). Monkeys had to fixate at one of three initial positions, hold fixation while a spatial cue was presented at one of eight target locations, and, after a memory period, make a saccade toward the cued target location. These eight potential target locations were arranged in a rectangle around the initial fixation point, with the same spatial arrangement relative to the fixation point for each of the three initial gaze positions (see Fig. 1*A* and MATERIALS AND METHODS). Because the monkeys were head-fixed in the straight-ahead direction, the position of the eyes in the orbit is equivalent to gaze direction.

A total of 268 units in the dorsal pulvinar were studied in two monkeys (*monkey C*: 86, *monkey L*: 182). For most analyses, beyond the effects during initial fixation we focused on the units with more than four trials for each combination of initial gaze and target position ($n = 238$; *monkey C*: 60; *monkey L*: 178; see MATERIALS AND METHODS). Normalized population PSTHs of these 238 units are displayed in Fig. 1*B*. In the population average there was no apparent dependence on the initial gaze position in the fixation hold epoch (note that the initial increase of the contralateral orange curve reflects visual/saccadic response to the onset of the fixation point in the contralateral hemifield). The enhanced contralateral cue response and bilateral postsaccadic enhancement are evident in the population.

The results in the two monkeys were consistent; therefore, we report the combined results from the entire sample. Sup-

plemental Tables S4–S13 provide numbers and proportions of units for various functional features separately for each animal. The example units (designated by lowercase letters "a" to "p") are referred to in figure legends and are summarized in Supplemental Table S14. Neurons in this sample exhibited diverse activity patterns; a summary of response modulation (enhancement or suppression) and spatial preferences across task epochs is given in Supplemental Fig. S3. In short, our sample contained 58% of units with initial fixation responses (29% enhanced, 29% suppressed, relative to pretrial "initialize trial" epoch), 41% with cue period activity (20% enhanced, 21% suppressed), 54% with memory delay period activity (17% enhanced, 37% suppressed), 23% with presaccadic activity (13% enhanced, 10% suppressed), and 65% with postsaccadic activity (48% enhanced, 17% suppressed); see Supplemental Fig. S3A and Supplemental Table S4. A detailed analysis of dPul neuronal response properties in a more extensive nonoverlapping sample is planned in a separate paper (see also Dominguez-Vargas et al. 2017). In this article, we focus on the activity patterns pertaining to different positions of the eyes in the orbit.

Gaze-Dependent Activity During Initial Fixation

A substantial portion of units (128 of 268, 48%) were significantly modulated by the gaze position before the cue was presented (one-way ANOVA). Many of these units maintained gaze dependence after cue presentation (47 of 128, 37%). Three example units shown in Fig. 2 illustrate tonic responses during the initial fixation and subsequent trial epochs. Focusing first on the initial fixation epoch, one example (Fig. 2*A*) shows contralateral gaze preference, and two other examples (Fig. 2, *B* and *C*) show ipsilateral preference. Our first question was if such gaze-dependent activity typically increased or decreased toward peripheral contra- or ipsilateral gaze positions, or if more units prefer the straight-ahead direction, as has been demonstrated in the visual cortex (Durand et al. 2010; Przybyszewski et al. 2014). To this end, we classified the units that showed a main effect of initial gaze position into units with monotonic gaze-dependent effects (showing peripheral preference) and units that showed either central or peripheral nonmonotonic gaze dependence (see MATERIALS AND METHODS).

Figure 3*A* shows normalized firing rates during fixation hold for each unit and each of the three initial gaze positions, grouped by the monotonicity and gaze direction preference. Monotonic responses were more frequent than nonmonotonic (91/128 and 37/128 units), but contralateral and ipsilateral preferences were almost balanced in monotonic units (41 and 50 units, respectively). Furthermore, in nonmonotonic units there was no bias toward the straight-ahead direction (18 vs. 19 units). Instead, we found an overall preference for peripheral positions (110 units: all monotonic and nonmonotonic peripheral gaze-preferring vs. 18 central gaze-preferring units). MR-guided reconstruction of recording sites revealed that units with significant gaze dependence were distributed throughout the sampled locations (mostly in the dorsal medial pulvinar), without a systematic clustering of gaze-dependent patterns (Fig. 3*B*).

Relationship Between Initial and Final Gaze Effects

Next, we evaluated the relationship between gaze-dependent activity during initial fixation and final fixation after the saccade (during target hold). Whereas those two periods are similar in terms of visuomotor requirements, we did this analysis because *1*) the latter period comes after an experimentally controlled saccade vector and might contain detectable traces of previous task stages, and *2*) it encompassed a wider range of gaze positions (±30° horizontally). Referring back to the examples in Fig. 2, the *units a* and *b* show mostly consistent contralateral or ipsilateral gaze preference throughout the trial. The *unit c* shows inconsistent gaze preference (contralateral for the initial gaze and ipsilateral after the saccade). To evaluate these patterns across the population, we compared gaze position preference in fixation hold and target hold epochs (Fig. 4*A*). Gaze position preference was computed as the difference of firing rate averages for contralateral and ipsilateral gaze positions (see schematics in Fig. 4*A*). Across all units, gaze position preference in the two epochs was positively correlated ($R = 0.3$, $P < 0.001$, Pearson's correlation), indicating a consistent effect of gaze direction irrespective of the task epoch. As expected, the correlation was mainly driven by units that show both an effect of initial and final gaze (significance derived from 2 independent one-way ANOVAs; $n = 91$, $R = 0.4$, $P < 0.001$). Figure 4*B* shows the results of the two independent ANOVAs. Only 29 units showed an effect of initial gaze but not final gaze position; conversely, 65 units showed only an effect of final gaze position. The high number of units with only an effect of final gaze might be due to a wider range of (final) gaze positions in the target hold epoch.

We next asked whether there is any influence of the initial gaze on activity associated with the final gaze after saccade. We performed a two-way ANOVA with the factors initial gaze and final gaze on firing rates in the target hold epoch, using the seven final target positions where the gaze would arrive from multiple starting points (schematic in Fig. 4*B*). The outer sectors of Fig. 4*B* display the number of units that showed a main effect of the final gaze and an interaction between initial and final gaze. Only 16% of units that showed an effect of final gaze position in the one-way ANOVA also showed an interaction between initial and final gaze in the two-way ANOVA (25/156), indicating that trial history (e.g., preceding saccade direction) did not have a major impact.

Because the final gaze covered more spatial locations (5×3), we assessed final gaze-dependent firing rate preferences in 2D space. Figure 4*C* shows color-coded histograms of gaze positions associated with maximum firing rates. Substantially more units preferred peripheral horizontal gaze positions as compared with central gaze positions (chi-square test, $P = 0.00021$ for all units, $P = 0.00235$ for units with significant final gaze position effect). This pattern is in agreement with the overall peripheral preferences during the initial fixation (cf. Fig. 3*A*). Interestingly, the distribution of firing rates on the population level was balanced across all final gaze positions (ranging from 13 to 15 spikes/s), similarly to the parietal cortex (Bremmer et al. 1998).

Given the sufficiently broad range of final gaze positions, especially in the horizontal dimension, we further quantified the monotonicity of the final gaze effects, separately for horizontal and vertical axes. We performed a two-way ANOVA

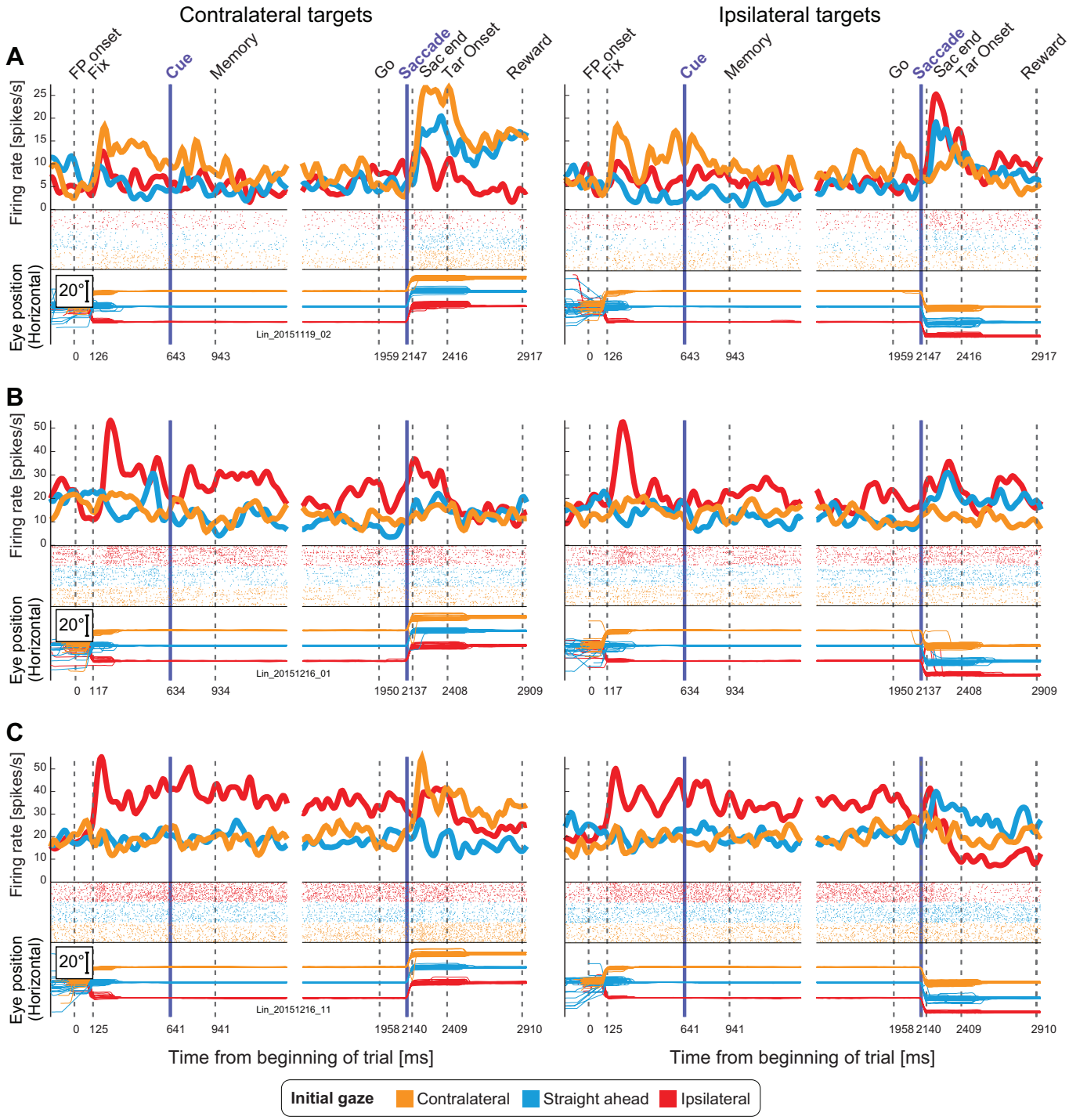

Fig. 2. Example units with tonic gaze-dependent activity. Raster plots, resulting spike density functions, and horizontal eye traces separately for each initial fixation position, for contralateral (*left*) and ipsilateral targets (*right*) relative to initial gaze position. Colors depict the 3 initial gaze positions (orange, contralateral; blue, straight ahead; red, ipsilateral). *A*: peripheral contralateral gaze preference (example *unit a*). *B* and *C*: peripheral ipsilateral gaze preference (*units b* and *c*, respectively). Vertical lines indicate average onset of events across all trials: fixation point onset (FP onset), the monkey acquiring fixation (Fix), the cue onset (Cue), the cue offset and beginning of the memory period (Memory), the offset of the central fixation point (Go), the saccade onset (Saccade), the monkey acquiring the invisible target location (Sac end), the onset of the confirmation target (Tar Onset), and the end of the trial (Reward). Discontinuous traces indicate 2 different alignments to cue onset and saccade onset (purple lines).

with factors horizontal and vertical final gaze position on target hold firing rates in all units that showed an effect of final gaze position in the one-way ANOVA ($n = 156$). Table 1 shows the numbers of units that exhibited main effects of horizontal/vertical gaze position, further separated into strict monotonic and nonmonotonic gaze preferences, independently for each axis (see MATERIALS AND METHODS). Most units (117/156, 75%) showed a main effect of horizontal gaze position, but only a minority showed strict monotonic gaze preference (32/117, 27%). Thus the wider range of five horizontal gaze positions

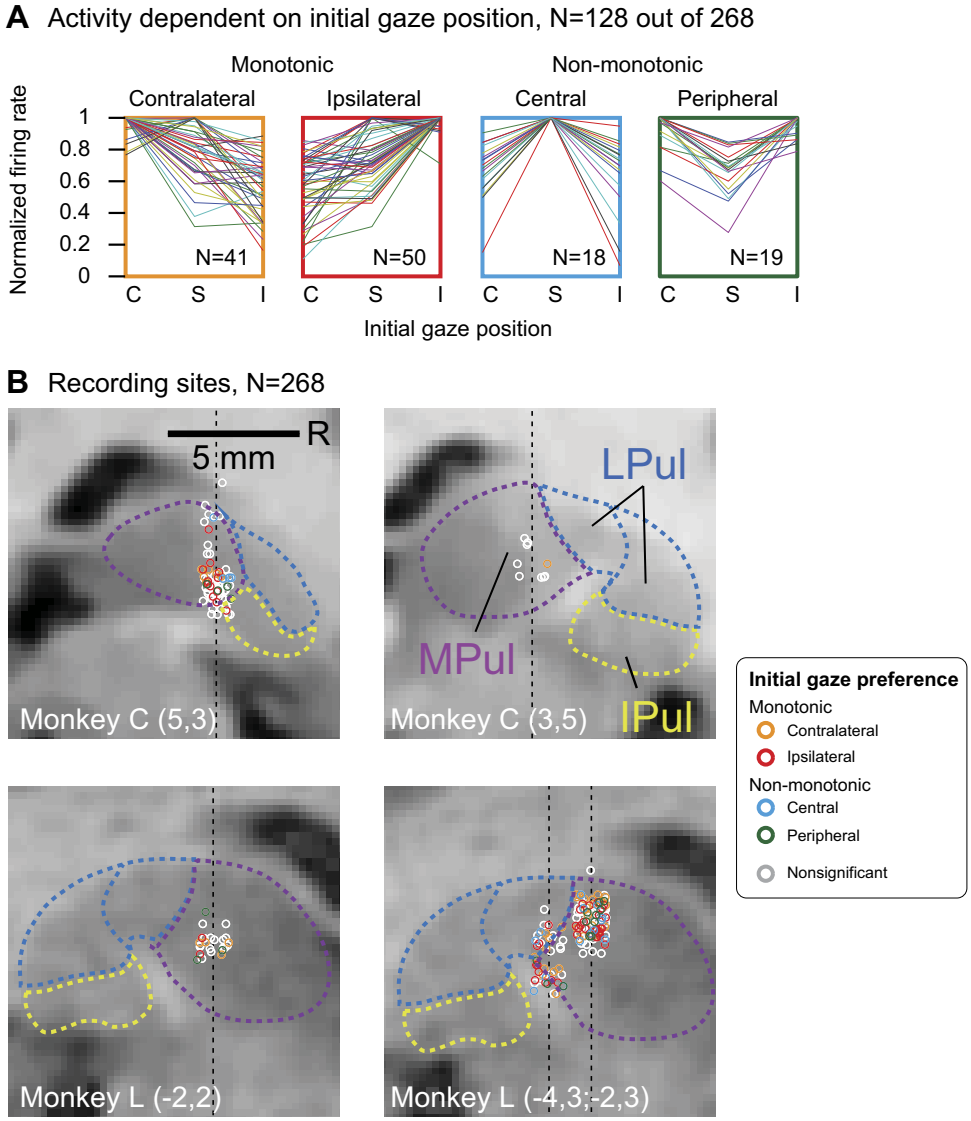

Fig. 3. Gaze dependence during initial fixation and recording sites. *A*: classification of initial gaze dependence. Data are normalized firing rates of each unit with a significant main effect of gaze on firing rates in the initial fixation epoch. Each line represents 1 unit. *X*-axis indicates initial gaze position: C, contralateral; S, straight ahead; I, ipsilateral. *B*: localization of recorded units in chamber-normal coronal sections in each monkey (*monkey L* and *monkey C*) and specific grid locations relative to the chamber center (*x*,*y* in parentheses). Locations were jittered along the horizontal dimension for better visualization. Black dashed lines indicate the projection of penetration tracks and mark the actual horizontal location of recorded neurons. Each circle represents 1 unit; colors indicate the initial gaze effects of the unit: orange for monotonic contralateral preference, red for monotonic ipsilateral preference, blue for central gaze preference, and green for nonmonotonic peripheral preference. Units that did not show a significant effect of gaze are shown in white. Pulvinar nuclei outlines (MPul/LPul/IPul, medial/lateral/inferior pulvinar) were adapted from the NeuroMaps atlas (Rohlfing et al. 2012), exported via Scalable Brain Atlas, https://scalablebrainatlas.incf.org/macaque/DB09 and https://scalablebrainatlas.incf.org/services/rgbslice.php (Bakker et al. 2015), and LPul was further subdivided into dorsal (PLdm) and ventral (PLvl) parts according to the brachium of the superior colliculus. See Supplemental Table S5 for data on individual monkeys.

(compared with only 3 initial gaze positions) revealed many units with nonmonotonic gaze dependence. Many units (87/156, 56%) also showed a main effect of vertical gaze position, and 71% of them showed monotonic vertical gaze preference (62/87). Altogether, 81/156 units showed monotonic dependence at least along one axis. A more detailed picture of final gaze preferences for each unit can be gained from Supplemental Fig. S4.

To utilize the 2D distribution of the 5 × 3 final gaze positions, and to account for potential saturation effects, we fitted final gaze dependent firing rates using three plausible 2D models: a linear, a sigmoidal, and a Gaussian model (see MATERIALS AND METHODS). We did not test a second-order polynomial model because the full model (U-shape or inverted U-shape) would be similar to a Gaussian, and a "half-branch" model (monotonic increase or decrease) to the sigmoidal model. Of 156 units that showed an effect of final gaze position, 25 were best fitted by the linear model, 61 by the sigmoidal model, and 55 by the Gaussian model, and 15 units were not significantly fitted by any of the models (Supplemental Fig. S5). This analysis is complementary to the analysis in the Supplemental Fig. S4, and some differences between the two approaches are expected: the nonmonotonic Gaussian model can only account for a single peak or trough, the fitting procedure may ignore local nonmonotonic variations, and in some cases the monotonic distribution of firing rates can be better fitted by a truncated 2D Gaussian. Nevertheless, considering the horizontal and the vertical axes separately or taking into account the 2D relationship of target locations produced a largely consistent account, with 52–55% of units showing a monotonic dependence and the remaining showing unimodal or complex nonmonotonic dependence. The correspondence between firing rates and 2D fits for each unit can be evaluated by comparing Supplemental Figs. S4 and S5. In agreement with the analysis in the Fig. 4*C*, the model fits also demonstrated only a handful of units with straight-ahead preferences (i.e., positive Gaussians with the peak near the center).

Time Course of Gaze-Dependent Modulation Around Saccades

To investigate if the eye position signals are updated predictively in the dorsal pulvinar, we applied the approach previously developed for studying the dynamics of eye position signals in the parietal cortex and in areas MT/MST (Morris et al. 2012). To this end, we subtracted the population signal

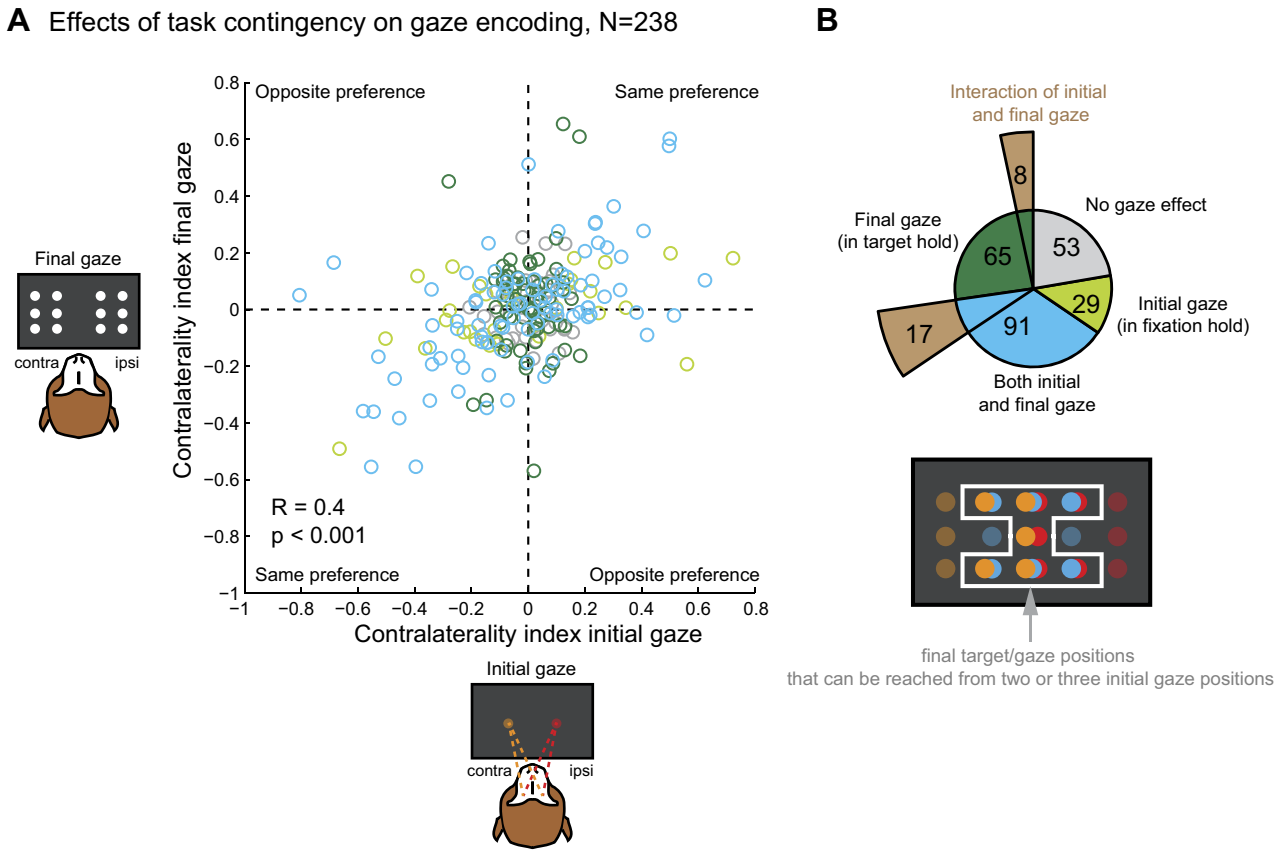

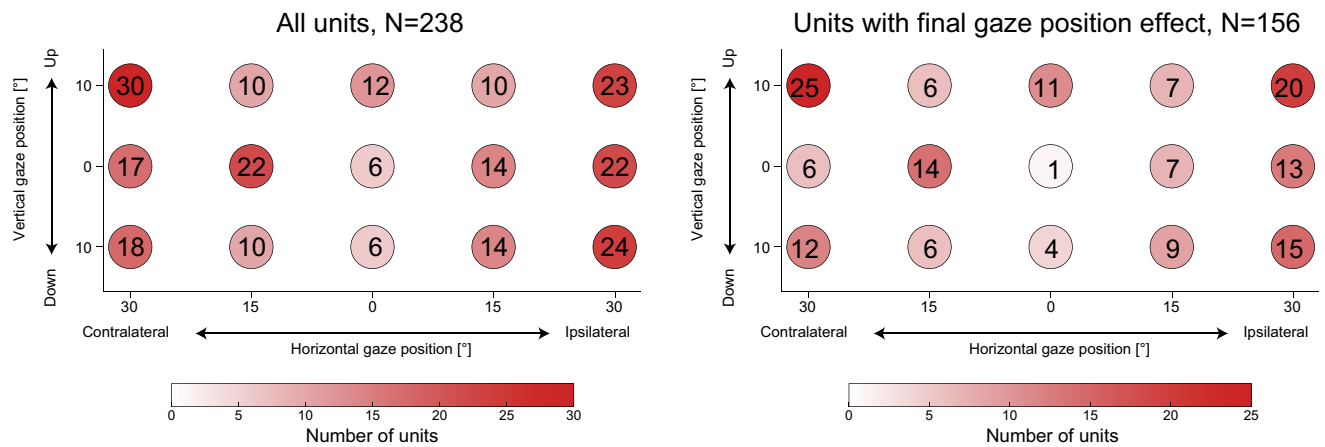

Fig. 4. Initial vs. final gaze-dependent activity. *A*: scatter plot of contralaterality indices denoting gaze direction preference in initial fixation (Fhol) vs. final target hold (Thol) epochs. Each circle represents a unit with at least 4 trials for every combination of initial gaze and retinocentric target position (n = 238). Contralaterality indices were computed as the difference of firing rates for contralateral (contra) and ipsilateral (ipsi) gaze positions, normalized by their sum. For the final gaze positions, 6 gaze positions in each hemifield were averaged (see schematic at *left*). Color of each unit depicts the combination of effects: significant initial gaze effect only (lime green), significant final gaze only (dark green), both initial and final gaze (cyan), or none (gray). Effects of initial and final gaze position were defined by 2 independent ANOVAs, testing firing rates in Fhol for initial gaze position and firing rates in Thol for final gaze position. *B*: ANOVA results. Inner sectors show the number of units in each group (same colors as in *A*), derived from the 2 independent 1-way ANOVAs (on initial and final gaze). Outer sectors indicate the number of units showing a main effect of final gaze as well as an interaction effect of the initial and the final gaze in the additional 2-way ANOVA that used only the highlighted (white border) target positions depicted in the schematic at the *bottom* (brown). See Supplemental Table S6 for data on individual monkeys. *C*: 2-dimensional histogram of final gaze preferences. Red color intensity indicates the count of units that showed the strongest response for the respective final gaze position (*left*, all units; *right*, only units showing significant effect of final gaze position). More units preferred peripheral positions (chi-square test, P = 0.00021 for all units, P = 0.00235 for units with significant final gaze position effect).

Table 1. *Patterns of final gaze dependence*

	Horizontal Axis		
Vertical Axis	Monotonic	Nonmonotonic	Nonsignificant
Monotonic	**13** (10)	**26** (13)	**23** (19)
Nonmonotonic	**5** (4)	19 (6)	1 (1)
Nonsignificant	**14** (12)	40 (16)	15 (5)

Data are the number of units exhibiting an effect of final gaze position (n = 156), grouped by significant monotonic and nonmonotonic main effects of horizontal and vertical gaze position (see Supplemental Fig. S4), with number of units best fitted by a monotonic linear or sigmoidal 2-dimensional model shown in parentheses (see Supplemental Fig. S5). Units that showed monotonic gaze dependence along at least one axis are in bold type (adding up to 81 units). See Supplemental Table S7) for data on individual monkeys.

derived from units that exhibited decrease in firing during postsaccadic fixation (NEG) from the signal derived from units that exhibited an increase (POS), using only the 156 units that showed an effect of final gaze position (see MATERIALS AND METHODS; Fig. 5). The resulting differential signal might represent the neural time course of the eye position signal (Morris et al. 2012). Unlike the signal in the cortex, we did not find predictive encoding of the upcoming eye position change around the saccade: the differential POS-NEG time course lags the saccade by 60–70 ms (Fig. 5). Note that the apparent "predictive signal" in Fig. 5*A* at the end of the memory period is a direct consequence of selecting units based on an increase or decrease of activity relative to this specific epoch; a similar artifact was discarded in the original study by Morris et al. (2012; see p. 178). Such artifact is also obvious in the Fig. 5*C*, where the initial fixation period, occurring long before the saccade (~1.5 s) and even before the upcoming target position is known, is taken as the "presaccadic epoch". To summarize, within the limits of our task design (memory-guided saccades as compared with visually guided saccades in the original study), the population of dorsal pulvinar neurons reflected the new eye position only after the saccade.

Gaze-Dependent Modulation of Spatially Contingent Task Epochs

So far, we had addressed the effect of gaze position on neuronal firing during either initial or final (target hold) fixation. Next, we asked how the retinocentric spatially contingent encoding is affected by gaze in the visual cue, memory delay, and saccadic epochs. We performed a two-way ANOVA with factors initial gaze position and retinocentric target location for each unit and each epoch of interest (Fig. 6*A*). During cue presentation, purely retinocentric encoding (only main effect of retinocentric target location) was less common than some dependence on the gaze position (41/238 vs. 82/238 units), indicating a strong influence of current gaze position on the response strength or tuning pattern. In the memory and perisaccadic epochs, purely retinocentric encoding became even less common (22/238 vs. 86/238 units and 25/238 vs. 50/238 units, respectively). It has been shown, for instance, in the parietal cortex that memory and perisaccadic responses are modulated by eye position (Andersen et al. 1990). The starting gaze position, however, can also influence saccade metrics (Barton and Sparks 2001), as was the case in our data (Supplemental Fig. S1 and Supplemental Table S1). Therefore, the influence of gaze on perisaccadic responses, which contain a mixture of oculomotor and visual reafferent signals, should be interpreted with caution.

One-third to one-half of the units showed an interaction of initial gaze position and retinocentric target location in the postsaccadic epochs (81/238 in the postsaccadic epoch and 114/238 in the target hold epoch). For an approximate estimation of the false discovery rate due to random firing fluctuations, we performed the same analysis on firing rates in the initial fixation epoch (where no information about target location was available to the monkeys). Whereas nearly half of the units showed only gaze-dependent activity during the initial fixation (108/238 units), only a small fraction showed a main effect of target location only (10/238 units), both main effects (6/238 units), or any combination with [initial gaze $\times$ target position] interaction (11/238 units), as expected.

The fraction of units with gaze dependence in the cue epoch decreased compared with that during initial fixation (120 vs. 82 of 238 units). Therefore, we asked if the arrival of the new spatial information overrode the initial gaze encoding in some neurons. Of 120 units that showed an effect of gaze position during initial fixation, 53 units maintained gaze dependence (main effect of gaze or interaction) in the cue epoch (and an additional 29 units acquired gaze dependence). Of 67 units that did not maintain gaze dependence, only 23 showed a main effect of retinocentric cue position, meaning that for the other 44 units, the loss of gaze encoding cannot be explained by replacement with new spatial cue information. Conversely, 22 of 53 units maintained gaze dependence despite additional encoding of the new retinocentric cue position. Supplemental Table S8 shows the data for individual monkeys. These findings together indicate that the decrease in gaze dependence was not related to cue responses. We also asked, more generally, if the units with the initial gaze effect were less likely to have visual cue responses. Table 2 shows that it was not the case: units with and without an effect of initial gaze position exhibited similar cue response patterns.

To get a better understanding of how gaze position affected visual responses, we looked into the cue epoch more closely. Example tuning curves for each category illustrate the combinations of gaze and cue dependence defined by the ANOVA (Fig. 6*B*). Some units showed a strong modulation by gaze position but no retinocentric cue tuning ("gaze only"), some showed the similar retinocentric cue tuning regardless of gaze position ("retinocentric cue only"; see also a more detailed example in Supplemental Fig. S6), some showed retinocentric cue tuning and an additive effect of gaze ("gaze and cue"), and some showed a multiplicative effect of gaze and/or an alteration of preferred retinocentric position by gaze ("gaze, cue, and interaction").

It should be noted that some units showed a clear response to the cue onset specifically for one gaze position, but no spatial cue tuning, as illustrated in the example shown in Fig. 6*C*. This finding demonstrates that cue responses may be underestimated when one looks at only one gaze position, and this should be considered in further studies assessing functional significance of cue responses in dorsal pulvinar.

Next, we tested if there is a relationship between gaze and spatial cue preference in units showing both types of dependence. We found no correlation between cue and gaze spatial preferences when correlating cue contralaterality indices (CIs)

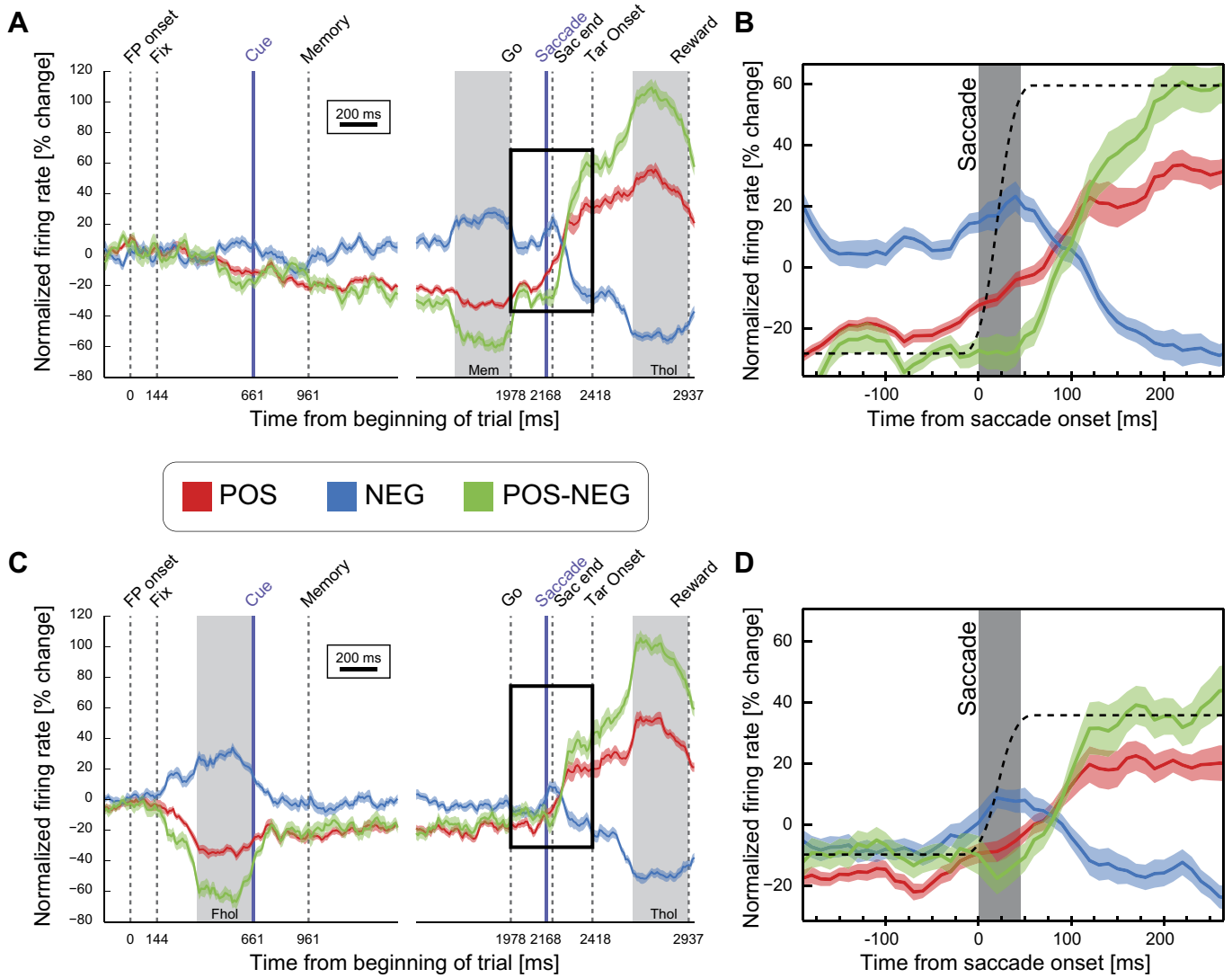

Fig. 5. Dynamics of eye position signals across saccades. Population activity is plotted separately for neurons that shift from a low to high firing rate (POS; red) and for units shifting from a high to low firing rate (NEG; blue) across successive fixations. The derived eye position signal, obtained by subtracting NEG from POS (POS-NEG) is shown in green (see MATERIALS AND METHODS for details). Vertical lines indicate average onset of events across all trials: fixation point onset (FP onset), the monkey acquiring fixation (Fix), the cue onset (Cue), the cue offset and beginning of the memory period (Memory), the offset of the central fixation point (Go), the saccade onset (Saccade), the monkey acquiring the invisible target location (Sac end), the onset of the confirmation target (Tar Onset), and the end of the trial (Reward). Discontinuous traces indicate 2 different alignments to cue onset and saccade onset (purple lines). *A*: POS and NEG derived using the memory period for presaccadic fixation (Mem; gray-shaded box) and the target hold for postsaccadic fixation (Thol; gray-shaded box). Here, 131 units contributed to POS and 98 to NEG, and in total 153 units contributed to the eye position signal POS-NEG. On average, 21 ± 1 units contributed to POS in each condition (i.e., a combination of initial and final gaze), 12 ± 1 to NEG, and 33 ± 2 to POS-NEG (means ± SE). *B*: magnified view of eye position signals around the saccade (black outline in *A*). Gray-shaded box indicates the duration of the saccade, and black dashed line indicates the timing of eye position scaled to match the step in firing rates. *C* and *D*: same as *A* and *B*, but using the initial fixation period (Fhol; gray-shaded box) for presaccadic fixation. Here, 124 units contributed to POS, 113 to NEG, and 153 to POS-NEG. On average, 17 ± 1 units contributed to POS in each condition, 15 ± 1 to NEG, and 32 ± 2 to POS-NEG.

to gaze CIs derived from the cue epoch ($R = -0.04$, $P = 0.513$, Pearson's correlation; see Fig. 6*D*), when correlating cue CIs with gaze CIs derived from the fixation hold epoch ($R = -0.05$, $P = 0.471$, Pearson's correlation), or when correlating raw (contra-ipsi) firing rate differences ($R = 0.05$, $P = 0.478$ for gaze in the cue epoch; $R = -0.03$, $P = 0.619$ for gaze in the fixation hold epoch). In fact, many units showed either hemifield preference of gaze position ($n = 56$) or retinocentric cue location ($n = 62$), but only a few units showed both ($n = 15$), with only six units showing the same hemifield preference.

To compare the strength of cue and gaze tuning, we computed absolute gaze and cue CIs and raw (contra-ipsi) firing rate differences and tested if there was a difference of the mean ranks (Wilcoxon signed rank test). There was no significant difference between the strength of cue and gaze tuning in any of the comparisons mentioned above [$P = 0.103$ for cue CIs and gaze CIs in cue, $P = 0.104$ for cue CIs and gaze CIs in fixation hold, $P = 0.2$ for raw firing rate differences (gaze in cue), $P = 0.295$ for raw firing rate differences (gaze in fixation hold)].

Modulation of Retinocentric Tuning by Gaze Position

Next, we focus on how gaze direction modulated units that showed retinocentric tuning. The motivation was to assess

whether gaze-dependent modulation would be consistent with gaze-dependent gain fields. The presence of such gain fields would indicate that the pulvinar participates in transformations between spatial reference frames using an efficient integration of visual and postural information. To this end, we bootstrapped the tuning vector (dependent on retinocentric target location) for each initial gaze position, independently for each unit and each epoch. To assess if gaze position amplified or shifted response fields, we computed confidence intervals for the estimated tuning vector for each gaze position and compared the confidence intervals around the mean for vector length and direction (see MATERIALS AND METHODS). This ap-

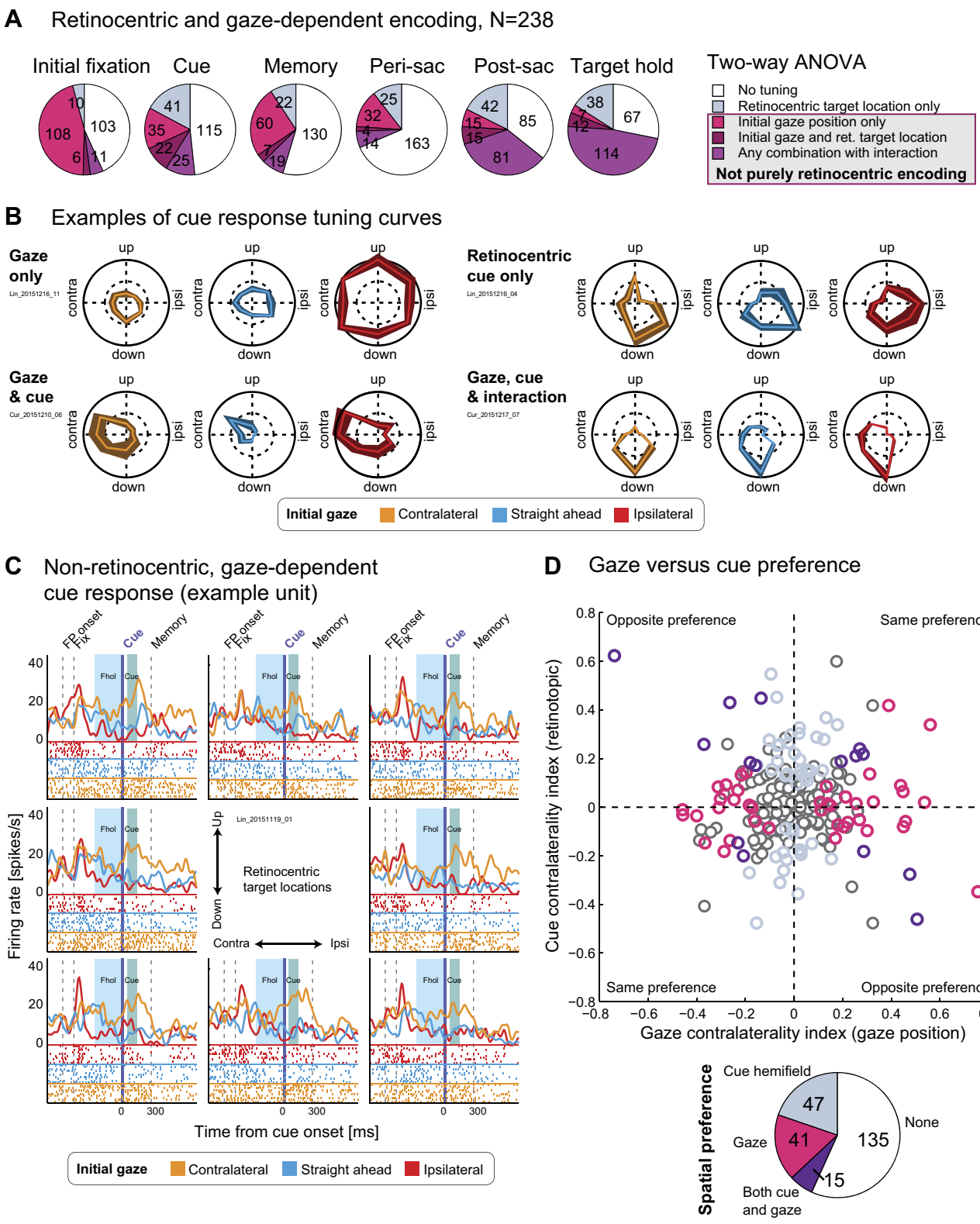

Table 2. *Relationship between initial gaze effect and cue responses*

Fixation Hold	Cue Response				No Cue Response
	Enhancement	Suppression	Hemifield preference	ANOVA position effect	
Initial gaze effect present	28	26	33 (26 with ANOVA position effect)	45 (17/13 en/su)	44
Initial gaze effect absent	20	24	29 (17 with ANOVA position effect)	30 (10/7 en/su)	55

Data are the number of units showing enhancement, suppression, hemifield preference, an effect of retinocentric position during cue presentation, or none of the above, given separately for units showing an initial gaze effect (in fixation hold; $n = 120$ units; cf. Fig. 4*B*, $120 = 91 + 29$) and for units showing no effect of initial gaze ($n = 118$). For position effect, en/su refers to the number of units in this group showing enhancement (en) or suppression (su). See Supplemental Table S9 for data on individual monkeys. Analysis of the relationship between initial gaze effect and saccade response is in Supplemental Table S10.

proach allowed us to assess changes in tuning without reliance on a specific tuning function. To illustrate this procedure, we modeled a neuron with a Gaussian retinocentric response field and a gaze-dependent linear multiplicative gain field and simulated recorded data for this hypothetical neuron by adding random noise for each trial (see Fig. 7*A*). Using this simulated data for bootstrapping the tuning vector for each gaze position and comparing confidence intervals of estimated tuning vector end points confirmed that the gain field properties of the modeled neuron could be reconstructed (see Fig. 7*B*).

Spatial firing rate patterns of six recorded example units exhibiting either gain field properties or response field shifts in the cue epoch are shown in Fig. 8*A*. For further illustration, PSTHs for each combination of initial gaze and retinocentric target location as well as the distribution of bootstrapped tuning vector end points are shown for the two example units in Fig. 8*A*, *top*. One example (Fig. 8*A*, *top left*) shows a classical gain field, with a retinocentric cue response amplified by gaze position. The other example (Fig. 8*A*, *top right*) shows a more complex pattern: the preferred location is modulated by the gaze position, with more ipsilateral gaze amplifying the central and upper contralateral cue response.

Figure 8*B* shows the number of units exhibiting a main effect of retinocentric target location (derived from two-way ANOVA in Fig. 6*A*), and of those units, the number of unit showing gain, shift, or both for each epoch. Among the epochs occurring before the saccadic eye movement, and thus reflecting the potential effects of the static gaze, we focus on visual cue responses. Of 75 units that showed a main effect of cue/target location, only 10 units (9 single units) showed a significant gain field component (7 monotonic). In those units, the gain amplitude was 66 ± 15% (mean ± SD; see MATERIALS AND METHODS). Importantly, our gain field analysis only detects the multiplicative impact of gaze on retinocentric tuning, which in the two-way ANOVA analysis (cf. Fig. 6*A*) would be reflected as a combination of the main effect of retinocentric target location and interaction (with or without the main effect of gaze). Indeed, 9 of the 12 units showing this combination were identified as showing significant gain field. The 22 units that showed main effects of retinocentric location and gaze but no interaction might be attributed to additive effects which are not defined as gain. The additive effect could be illustrated by the tuning curves of the example unit in Fig. 6*B* ("gaze and cue").

The interpretation of the two postsaccadic epochs (immediately after saccade and during target onset) is more complicated because gaze-dependent effects could also reflect the final gaze position (which is not fully dissociated from the initial gaze position). In fact, 46 of 53 units showing gain and/or shift in the postsaccadic epoch and 42 of 45 units showing gain and/or shift in the target onset epoch also show an effect of final gaze position in the same epoch, making gaze position encoding the most parsimonious explanation for the relatively frequent gain and shift effects in these epochs.

As a control, we also performed this analysis on firing rates during fixation hold to get an estimate for the false discovery rate due to random fluctuations (because at that point there was no difference between trials with different retinocentric target locations). Only one unit showed a spurious "shift" effect, suggesting that the findings in other epochs are not due to random noise fluctuations.

Reference Frame Evaluation

Finally, we evaluated in which reference frame dPul neurons encode spatial information. Because the monkey's head position was always fixed straight ahead relative to the screen, and we did not control for the trunk rotation in the chair (although typically the trunk was facing the screen), we cannot dissociate between head-, body-, or world-centered representations. How-

Fig. 6. Retinocentric and gaze-dependent encoding. *A*: 2-way ANOVA results, with factors initial gaze position and retinocentric target location, independently for 6 epochs: fixation hold (Fhol), cue onset (Cue), memory (Mem), perisaccadic (Peri), postsaccadic (Post), and target hold (Thol). Pie plots show the number of units showing either only a main effect of retinocentric target location, only a main effect of initial gaze position, both main effects, or any combination with [initial gaze position × retinocentric target location] interaction (plus no main effect, both main effects, or one of the two main effects). For brevity, the presaccadic epoch is omitted because the numbers were nearly identical to those for the perisaccadic epoch, and the target onset epoch is omitted because the numbers were nearly identical to those for the postsaccadic epoch. *B*: polar plots of retinocentric cue responses for each gaze position (contra, contralateral; ipsi, ipsilateral). One example unit from each category in the 2-way ANOVA: gaze only (*unit c*), gaze and cue (*unit d*), retinocentric cue only (*unit e*), gaze, cue and interaction (*unit f*). *C*: peristimulus time histograms and raster plots of activity around the cue onset for 1 example unit (*unit g*) showing a main effect of gaze (in the cue epoch) only, separately for each retinocentric cue location (in different subplots) and each gaze position (in different colors). Vertical lines indicate average onset of events around he cue onset: fixation point onset (FP onset), the monkey acquiring fixation (Fix), the cue onset (Cue), and the cue offset and beginning of the memory period (Memory). Purple lines indicate alignments to cue onset. *D*, *top*: scatter plot of cue and initial gaze contralaterality indices. Colors indicate significant hemifield preferences (light blue, cue; magenta, gaze; purple, both cue and gaze; gray, no hemifield preferences). *Bottom*: pie plot showing the number of units with hemifield preferences for cue, gaze, both, or none. See Supplemental Table S11 for data on individual monkeys.

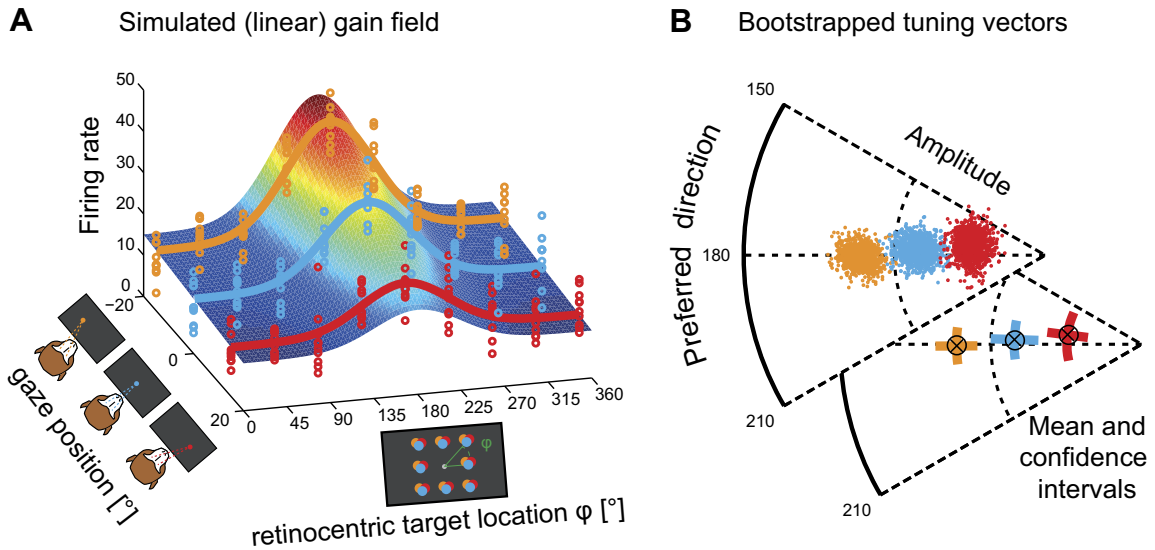

Fig. 7. Tuning vector bootstrapping approach. *A*: 3-dimensional plot of a simulated gain field. Each color corresponds to one initial gaze position. Firing rates were simulated using a Gaussian tuning curve (dependent on retinocentric target location φ, preferred direction = 180°), which was amplified by the initial gaze position. Noise was added to create variability for each trial (colored circles). To illustrate the comparison with the results derived from the 2-way ANOVA with factors retinocentric location and gaze position, such gain field results in both main effects and interaction. *B*: population vectors for each initial gaze position were bootstrapped (see MATERIALS AND METHODS) to compute confidence intervals for amplitude and direction of the estimated population vectors for each initial gaze position.

ever, we can dissociate these three possibilities from retinocentric (i.e., eye centered) representations. For simplicity, in the following text a "screen-centered" reference frame refers to a potential head-, body-, or world-centered reference frame, as opposed to a retinocentric one.

To evaluate if response patterns were better explained by retinocentric or screen-centered representations, we compared the alignment of responses in retinocentric and screen-centered coordinates for seven task epochs, following a previously applied approach (see MATERIALS AND METHODS; Mullette-Gillman et al. 2005). For this analysis, we included only units that exhibited a dependence on target locations in any reference frame: i.e., only units that showed either a main effect of retinocentric target location, [retinocentric location × initial gaze] interaction, a main effect of target location on the screen, or [screen location × initial gaze] interaction. In Fig. 9, each data point represents the average correlation coefficient (ACC) between the unit's responses for different initial gaze positions when locations were defined relative to the eye (retinocentric ACC, horizontal axis) and relative to the screen (screen-centered ACC, vertical axis). Units above the diagonal indicate better alignment of responses in screen-centered coordinates, and units below the diagonal indicate better alignment in retinocentric coordinates. Figure 9 shows a progression from prevalence of units compatible with retinocentric reference frames in the cue epoch to screen-centered encoding in the target hold epoch, with a balanced representation immediately after the saccade. This indicates that visual responses and/or movement preparation were encoded in retinocentric coordinates, whereas the new gaze position was the predominant factor encoded in postsaccadic epochs. As additional support for this interpretation, we performed paired *t* tests comparing retinocentric ACCs and screen-centered ACCs across all included units in each epoch, showing significantly stronger retinocentric alignment in the cue ($P < 0.001$), memory ($P = 0.01$), and perisaccadic epochs ($P = 0.001$) and stronger screen-centered alignment in the target onset ($P = 0.003$) and target hold epochs ($P < 0.001$). Two example units with screen-centered reference frames in target hold are shown in Supplemental Fig. S7.

Apart from the units that could be classified as retinocentric or screen centered, in each epoch, many units showed mixed, or hybrid, encoding that cannot be more strongly attributed to either of the two references frames (Caruso et al. 2018). Many of these units had high ACCs in both frames; i.e., the both reference frames could account for the observed response functions. To illustrate this, we show an example unit that responded predominantly to upper targets and had high ACCs in both reference frames (e.g., 0.84 for screen-centered units and 0.81 for retinocentric units in the memory epoch), making it difficult to dissociate the two (Supplemental Fig. S8). This and other mixed units showed response patterns that are consistent with a partial shift of response function with the eye position (Caruso et al. 2018).

Finally, to demonstrate that our findings are not confounded by combining units with different properties within multiunits, we also performed several analyses on single units only, leading to comparable results (see Supplemental Fig. S9).

DISCUSSION

The dorsal pulvinar has been implicated in spatial processing supporting goal-directed eye movements, but so far the implicit experimental assumption has been that it encodes space in retinocentric (eye centered) coordinates, even if it does not show a retinotopic organization (i.e., gradual topographic representation of visual space across adjacent regions of neural tissue). In the present study we show that many dorsal pulvinar neurons are influenced by the position of the eyes in the orbit (equivalent to the gaze direction, when the animal's head is immobilized), in two different ways. First, in more than half of the sample, the firing during steady fixation of a foveal stim-

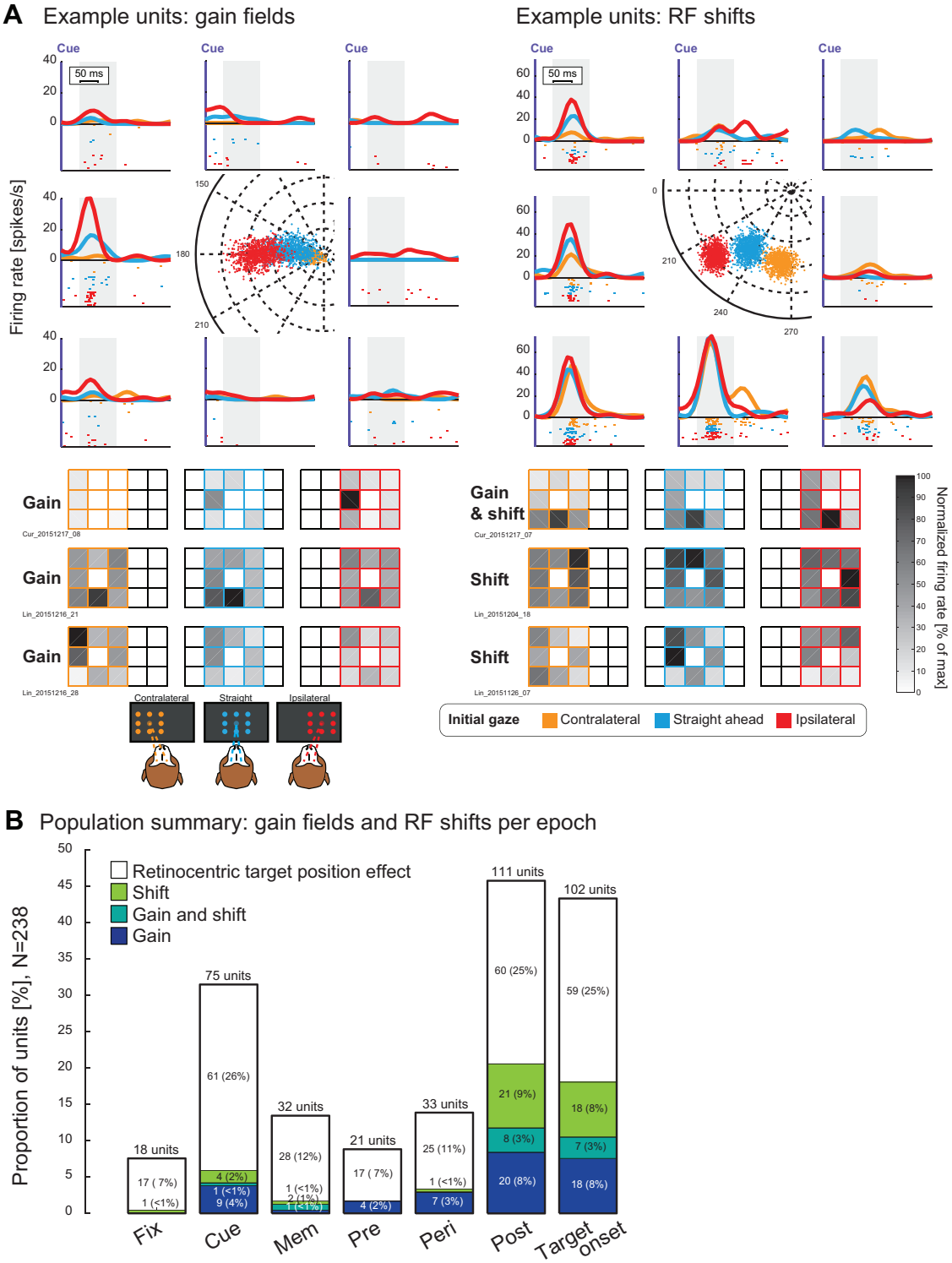

Fig. 8. Gain field and response field (RF) shift properties. *A*: example units showing gain field properties (*left*) or RF shifts (*right*) in the cue epoch. *Top*: peristimulus time histograms (PSTHs) during cue presentation for each of the initial gaze positions and each of the retinocentric target locations, spatially arranged according to the retinocentric location (*left*, *unit h*; *right*, *unit f*). In the center of the PSTH plots, the corresponding bootstrapped population vector end points for each initial gaze position are displayed. *Bottom*: heat map plots of the example units shown in PSTHs (*top left* row) and 2 additional examples showing either gain field properties (*middle left* row *unit I*; *bottom left* row, *unit j*) or RF shift properties (*middle right* row, *unit k*; *bottom right* row, *unit l*). *B*: number of units showing a main effect of retinocentric target position (above bar), and of those, the number (and percentage) of units showing gain field (blue) or RF shift properties (green) for each epoch of interest. Units showing both effects (cyan) and units showing only an effect of target position (open portion of bars) are also displayed. Fixation hold (Fix) epoch was added as a control to approximate the expected statistical noise level. See Supplemental Table S12 for data on individual monkeys. Cue, cue onset epoch; Mem, memory epoch; Peri, perisaccadic epoch; Post, postsaccadic epoch.

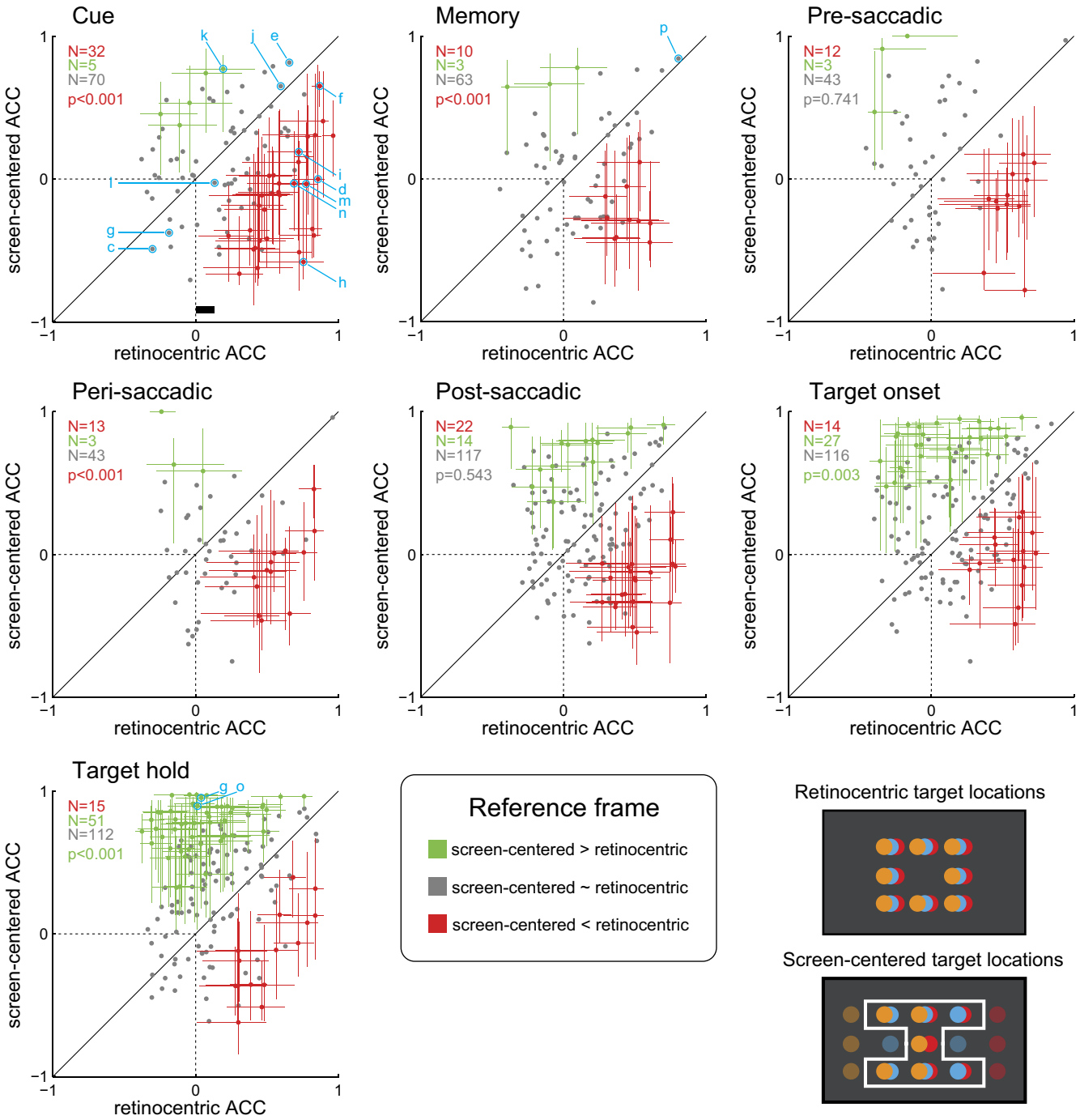

Fig. 9. Reference frame evaluation. Average correlation coefficients (ACCs) in retinocentric coordinates (*x*-axis) and screen-centered coordinates (*y*-axis) for each unit in 7 epochs of interest: cue, memory, presaccadic, perisaccadic, postsaccadic, target onset, and target hold. Crosshairs indicate 95% confidence intervals derived from bootstrapping. Note that dots represent actual ACCs calculated using all data, and their location is not necessarily centered in the middle of the confidence intervals. Units where the crosshair is above the diagonal (and >0 on the *y*-axis) were classified as "more screen-centered than retinocentric" (green), and units where the crosshair is below the diagonal (and >0 in the *x*-axis) were classified as "more retinocentric than screen-centered" (red); see MATERIALS AND METHODS for details. For the remaining units (mixed, or hybrid encoding; gray), confidence intervals were omitted for clarity. For eye-centered correlations, all 8 target locations were used; for screen-centered correlations, only overlapping target locations for each specific correlation pair were used (7 targets outlined by the white frame, *bottom right*). *P* values indicate significance of paired *t* tests comparing screen-centered and retinocentric ACCs across all included units; text color indicates which was larger (in case of significant differences). See Supplemental Table S13 for data on individual monkeys. For cross-referencing, we labeled the example units appearing in other figures, except *units a* and *b*, which appear only in Fig. 2; see Supplemental Table S14 for the list of all example units.

ulus was influenced by the gaze direction. Second, depending on the epoch, substantial numbers of neurons showed a combination of retinocentric and gaze-dependent signals in visual and saccadic responses to a peripheral stimulus, and some of these effects could be described as gaze-depended gain modulation. The analysis of reference frames across consequent task epochs, from cue to postsaccadic target hold, indicated a transition from predominantly retinocentric encoding to coding

of final gaze or target location in head/body/world-centered coordinates. Despite some limitations in the current study design (see below), these results provide electrophysiological evidence to support the previously hypothesized notion that the dorsal pulvinar might contain neurons that reflect postural signals and represent space in nonretinocentric reference frames (Grieve et al. 2000). In the following, we relate our findings to the previous cortical and thalamic literature, separately discussing the influence of eye position on ongoing firing during foveal fixation and on visuomotor representations of peripheral targets.

Comparison to Previous Electrophysiological Studies in the Thalamus

Previous electrophysiological studies in the central thalamus of monkeys have reported neural activity modulation by eye position in the orbit (Schlag-Rey and Schlag 1984; Tanaka 2007; Wyder et al. 2003). Similar to the dorsal pulvinar, the central thalamus is a "higher order" nucleus complex with connections to cortical regions, such as frontal and supplementary eye fields and posterior parietal cortex, that are crucial for oculomotor behaviors (Tanaka and Kunimatsu 2011). The central thalamus also receives afferent inputs from the cerebellum and oculomotor brain stem involved in eye movement control.

In respect to effects of eye position on ongoing fixation activity, a study in the central ("oculomotor") thalamus reported few neurons showing an influence of gaze on sustained postsaccadic activity, either increasing or decreasing monotonically with the contralateral gaze eccentricity (Wyder et al. 2003). In our sample, about half of dPul units that were affected by the final (postsaccadic) gaze position exhibited monotonic dependence.

Another study that focused on eye position responses in the central thalamus also found, in addition to transient postsaccadic responses, many neurons with sustained postsaccadic firing modulated by eye position, mostly along the horizontal axis (Tanaka 2007). Some neurons also showed a "memory trace" of the preceding saccade; i.e., the activity at the same final position depended on where the eye came from. Such a hysteresis effect was also reported in the central thalamus during spontaneous eye movements (Schlag-Rey and Schlag 1984). This is reminiscent of our subset of neurons showing an interaction between the initial and the final gaze position after the saccade. However, unlike our findings, the central thalamus neurons could be divided into two main groups: neurons that showed predictive presaccadic tuning corresponding to the final gaze position, and those that were modulated by the gaze only after the saccade (Tanaka 2007). In our sample, the majority of neurons were similar to the latter group, whereas the units showing presaccadic responses consistent with encoding the upcoming postsaccadic gaze were exceedingly rare. The population-derived eye position signal did not have a predictive component and was delayed relative to the saccade.

The thalamus literature on gaze-dependent modulation of eccentric visual responses (e.g., potential gain field effects) is sparse. The modulation of visual responses by the (passive) eye position has been reported in lateral geniculate nucleus (LGN) of anesthetized cats (Lal and Friedlander 1989). The eccentric visual responses in the cat internal medullary lamina (IML) were found to be related to a confluence of a specific retinocentric direction and a target area defined in screen/head/body-related coordinates, determined by spontaneous gaze locations (Schlag et al. 1980). In the retinotopically organized macaque ventral pulvinar, visual sensitivity of a small subset of neurons to stimuli flashed in the receptive field at different times around the saccade was influenced by orbital position (Robinson et al. 1990). Apart from those pioneering studies, to our knowledge there has been no systematic assessment of potential gaze-dependent gain fields in higher order thalamus.

Comparison to Previous Electrophysiological Studies in Cortex

Eye position effects in cortex were mostly considered in the context of reference frame transformations and integration of sensory information into head- and body-centered coordinates. Nonetheless, the studies that have tested the influence of gaze on ongoing activity during fixation (even in the dark) also reported eye position-dependent effects. Specifically, eye position signals during fixation have been reported in many cortical areas, including visual (V1–V4, medial temporal area MT, MST) (Bremmer 2000; Morris et al. 2013; Morris and Krekelberg 2019; Rosenbluth and Allman 2002; Trotter and Celebrini 1999), posterior parietal (LIP, MIP, 7a, VIP, V6) (Andersen et al. 1990; Andersen and Mountcastle 1983; Bremmer et al. 1997; Galletti et al. 1995; Genovesio et al. 2007; Mullette-Gillman et al. 2005; Sakata et al. 1980), dorsal premotor (Boussaoud et al. 1998), and somatosensory cortex (Wang et al. 2007). Below we briefly discuss a number of particularly pertinent studies.

Sakata et al. (1980) studied neurons in area 7a, LIP, and MST that were driven by gaze direction ("visual fixation neurons", ~11% of the total sample). The majority (86/125) of visual fixation neurons varied systematically with gaze angle in the frontal plane. Many of those neurons were also selective for depth of fixation. These results are broadly consistent with later studies in areas LIP and 7a, where subpopulations of neurons were reported to exhibit tonic background activity during fixation that varied monotonically with eye position without showing any visual responsiveness (Andersen et al. 1990). Similarly, another study in LIP and 7a reported an influence of eye position during visual fixation in darkness with about a third of neurons that could be best fit with a monotonic (linear) regression model (Bremmer et al. 1997). A comprehensive study that compared how well eye position signals during fixation can be decoded from neurons recorded from LIP, VIP, and visual areas MT and MST concluded that eccentric fixations could be decoded more accurately than central ones and that LIP/VIP populations encode eye position more accurately than visual cortex (Morris et al. 2013). Another study in the same brain areas showed that eye position signals are updated predictively and might contribute to perceptual (mis)localization around the saccade (Morris et al. 2012). A similar analysis in dPul did not reveal a predictive component, suggesting that the eye position signals in dPul are not a mere copy of the dynamics in its cortical partners, and vice versa.

Eye position signals that were monotonically related to the eccentricity of gaze were also reported in primary somatosensory cortex S1 (Wang et al. 2007; Xu et al. 2011). This study concluded that those eye position signals in S1 had a proprio-

ceptive origin given that anesthetizing the contralateral orbital muscles nearly abolished the recorded eye position signals. Similarly, a preference for more eccentric eye positions was reported in parietal cortex (Sakata et al. 1980). Although a study in parietal cortex reported a fairly balanced distribution of firing across different fixation positions on the population level, this was due to almost equal ratios of "leftward vs. rightward" and "up vs. down" planar slopes, rather than an equal proportion of peripheral and central preferences in individual neurons (Bremmer et al. 1998). In the dPul we also found a predominance of peripheral gaze preferences, using both firing rates and 2D model fitting approaches.

Although the relationship between gaze-dependent effects during fixation and peripheral target encoding has been rarely explicitly discussed, it can be inferred from studies in parietal and premotor cortex that all three categories are typically observed: namely, *1*) neurons that are modulated by the gaze during fixation but are not responsive in subsequent task epochs, *2*) neurons that only show modulation of visual/delay/saccade responses by gaze, and *3*) neurons that show both types of gaze dependence. Similarly, we found all three categories in dPul, and no systematic relationship between presence or absence of gaze dependence and visual cue responses.

The majority of studies on eye position signals in cortex focused on the second aspect of gaze dependence: modulation of visual, motor planning, and saccade-related activity in response to peripheral targets (Lehky et al. 2016). Specifically, when a neuron changes its response to a stimulus depending on eye position while the retinal location remains the same, this pattern has been described as eye position gain field. Computational models applied to the response modulation of single neurons in parietal (Andersen et al. 1990) and visual cortex (Bremmer 2000) have often modeled the gain fields as planar, or at least monotonic (Pouget and Sejnowski 1997; Zipser and Andersen 1988). It needs to be noted, however, that even in posterior parietal cortex, the proportion of neurons reported to exhibit planar gain fields was only 39% (Andersen et al. 1985), and multidimensional scaling methods applied to neuronal populations in the lateral intraparietal cortex (LIP) and anterior inferotemporal cortex to infer current eye position show that other, nonlinear functions (e.g., sigmoidal, elliptical, or hyperbolic, or complex mixtures of thereof) might fit the data as well (Lehky et al. 2016). Likewise, eye position gain fields of neurons in area V6 (PO) have diverse shapes from planar to peak shaped (Galletti et al. 1995). Similarly to those findings, in the current study the gain fields in dPul appeared to be a mixture of monotonic and peak-shaped fields (but given only the 3 initial gaze positions we used, those conclusions are tentative). This is unlike the primary visual cortex, where the straight ahead direction typically has stronger gain, leading to mainly peak-shaped fields (Durand et al. 2010; Przybyszewski et al. 2014).

In addition to the modulation of retinocentric encoding by eye position, several other oculomotor studies also reported encoding of visual/saccade targets in other reference frames, e.g., head-centered or mixed, or hybrid, coordinates (Brotchie et al. 1995; Caruso et al. 2018; Galletti et al. 1995; Mullette-Gillman et al. 2005). Apart from a retinocentric reference frame, we also observed a small subset of neurons that were more consistent with head/body/world-centered encoding before the saccade and many neurons with mixed encoding. For instance, some units showed (not tuned retinocentrically) visual cue responses only at certain gaze positions (cf. Fig. 6*C*). Because the eye position could determine whether there was a visual response at all, it is conceivable to construe those neurons as primarily encoding eye position that is modulated by a visual response as opposed to the typical concept of eye position "gain fields" where the visual response is modulated by eye position.

In our data, the prevalence of significant eye-centered encoding in cue, memory, and presaccadic epochs is supplanted soon after the saccade by head/body/world-centered reference frame encoding, which can also be interpreted as the encoding of the current gaze. This finding is in line with ANOVA results showing the final gaze/target encoding during late postsaccadic fixation. The transition from retinocentric target to gaze position encoding in dPul resembles a recent study in FEF, with the difference that the transition happens after the saccade in dPul, compared with the predictive presaccadic transition from retinocentric target code to (also retinocentric) motor goal in FEF (Sajad et al. 2016). The immediate postsaccadic epoch in dPul still contained units with retinocentric encoding, akin to eye movement vector postsaccadic encoding in LIP, which dissipated in the late postsaccadic period (Genovesio et al. 2007). A small subset compatible with retinocentric encoding during target hold, long after the saccade, was unexpected, but the visual inspection confirmed that those units indeed retained a trace of the retinocentric saccade vector.

Possible Sources of Eye Position Signals in Dorsal Pulvinar

Given the extensive connectivity of the dorsal pulvinar to parietal and premotor cortex, and partial resemblance of eye position-dependent effects in those areas and in dPul, one likely possibility is that the eye position effects in dPul are inherited from those visuomotor areas (Cappe et al. 2007, 2009; Romanski et al. 1997; Schmahmann and Pandya 1990; Yeterian and Pandya 1989). The source of continuous eye position signals in the cortex is still not fully identified (Xu et al. 2012; Ziesche and Hamker 2011). One possibility is the corollary discharge of the motor command that maintains steady eye position (Morris et al. 2012; Xu et al. 2012), counteracting the elastic elements of the orbital tissues (Sylvestre and Cullen 1999). Another candidate is the proprioceptive signal reflecting the current position of the eyes in the orbit (Wang et al. 2007). The dPul can receive this signal from parietal and premotor areas, and/or directly from the primary somatosensory cortex (Wang et al. 2007; Xu et al. 2011), given medial pulvinar connectivity to area 3a (Padberg et al. 2009). This possibility could be investigated further by anesthetizing the extraocular muscles (Wang et al. 2007) or by inactivating the projection from somatosensory area 3a and recording in the dPul.

Yet another possibility, which would place dPul as a potential source of eye position signals to the cortex, is the corollary discharge via superior colliculus-pulvinar-cortical pathway (Guthrie et al. 1983; Wurtz et al. 2011a). Dorsal pulvinar, including the lateral portion of the medial pulvinar where our recordings were mainly performed, receives afferents from the intermediate and deep layers of the superior colliculus (Baldwin and Bourne 2017; Bender and Butter 1987; Benevento and Standage 1983; Harting et al. 1980). The intermediate and deep

layers of SC exhibit eye position dependence, including gain fields (Campos et al. 2006; Van Opstal et al. 1995). It has been shown that in addition to the proprioceptive information about eye position, a preparatory corollary discharge/efference copy of planned saccade, originating in the superior colliculus and routed to frontal cortex via mediodorsal thalamus (MD), can carry eye position signals (Crapse and Sommer 2008; Wurtz et al. 2011a). Similarly, it has been suggested that the dorsal lateral pulvinar might carry preparatory movement-related signals to parietal cortex (Wurtz et al. 2011b), although those signals might only be relevant around the time of a saccade.

Although anatomical projections of the superior colliculus to the dPul have been reported (but see Zhou et al. 2017), there is a debate on specificity of projections to medial vs. lateral pulvinar and on their functional impact (Baldwin and Bourne 2017)). The functional contribution of projections from SC is more studied in the ventral pulvinar. Specifically, extensive lesions of SC caused only little effect on visual responses in the ventral pulvinar, compared with striate cortex lesions (Bender 1983). In rabbits, however, the inactivation of SC led to a strong attenuation of responses in lateral posterior (LP) nucleus (which is a part of the LP-pulvinar complex in nonprimate species: mice, rats, rabbits, cats, and tree shrews) (Casanova and Molotchnikoff 1990). Furthermore, selective microstimulation of the superficial layers of the SC in macaques elicits (monosynaptic) responses in the ventral pulvinar (Kinoshita et al. 2019), in agreement with earlier work that identified the projection from SC to area MT via ventral pulvinar (Berman and Wurtz 2011). Extrapolating from these ventral pulvinar studies to the dorsal pulvinar, the potential influence of SC inputs to dPul (Wurtz et al. 2005) might be outweighed by more extensive cortical driving inputs (Bickford 2016; Rovó et al. 2012). To fully elucidate complex cortico-pulvinar-cortical loops and subcortical inputs to pulvinar, it would be crucial to manipulate the specific projections from and to the pulvinar, using pathway-selective techniques such as optogenetics and/or viral vectors (Kinoshita et al. 2019; Schmitt et al. 2017).

Pulvinar also receives projections from pretectal nuclei (Benevento and Standage 1983; Schmidt et al. 2001). These nuclei have oculomotor functions related to optokinetic nystagmus and smooth pursuit and show visuomotor activity resembling pulvinar responses (Sudkamp and Schmidt 2000). Therefore, pretectum could also be a source of eye position signals.

Apart from cortex and midbrain, another possible source of eye position signals in the pulvinar is the cerebellum. The cerebellum is involved in a number of eye movement control functions, including maintenance of steady fixation, smooth pursuit, and binocular alignment (Krauzlis et al. 2017; Patel and Zee 2015). To our knowledge, no study in monkeys or humans has described (monosynaptic) pathways between dorsal pulvinar and cerebellum. In cats, several earlier histological labeling studies described projections from the cerebellum to the contralateral LP nucleus (Itoh and Mizuno 1979; Rodrigo-Angulo and Reinoso-Suarez 1984). These cerebello-LP projections in cats overlap with the ones coming from the deep layers of the superior colliculus and other brain stem nuclei. It is not clear, however, whether these results can be extrapolated to the medial portion of the dorsal pulvinar, which is only fully developed in primates (Jones 2007; Preuss 2007). Some evidence (albeit not necessarily for a monosynaptic pathway) can be derived from microstimulation of the cerebellum in monkeys showing evoked blood oxygenation level-dependent (BOLD) functional MRI activity in the dorsal pulvinar (Sultan et al. 2012). Indirect evidence for a functional connection could also be derived from a recently described human patient with a circumscribed (bilateral) lesion in the medial pulvinar who exhibited a mixture of parietal and cerebellar neurological deficits (Wilke et al. 2018). Being somewhat speculative, the anatomical and functional connectivity between pulvinar and cerebellum in primates needs to be studied in more depth.

Methodological Limitations and Future Directions

In our experiments, as in many previous studies, the head was immobilized in the straight-ahead direction relative to the body and the center of the screen. Hence, head-, body-, or world (screen)-centered references cannot be dissociated in this design (Mullette-Gillman et al. 2005). Because of the same limitation, when interpreting the modulation of responses during fixation at initial or final gaze positions, we cannot distinguish between encoding of eye position in the orbit (e.g., via a proprioceptive signal) vs. spatial representation of the fixated stimulus (in any of the above reference frames).

In our design, only 7 of 15 final gaze positions resulted from different initial gaze positions, and hence different saccade vectors, limiting the statistical power for dissociating the postsaccadic vector encoding from effects of postsaccadic eye position. Furthermore, we only varied the initial horizontal gaze position. A hypothetical extreme example of a purely retinocentric encoding with postsaccadic responses for all upper targets would also result in an apparent upper final gaze preference with the same "goodness of fit," demonstrating that in some cases those two encoding schemes cannot be dissociated. Therefore, at least partially, the final gaze encoding could be a result of "tiling" retinocentric (saccade vector) response fields originating from the three initial gaze positions. Several lines of evidence in our data, however, suggest that the static position of the eyes in the orbit is the defining factor in postsaccadic tuning, especially in the later part of the postsaccadic epoch. First, the corresponding target hold epoch analyzed in this study started 400 ms after the saccade end. Second, the two-way [initial gaze $\times$ retinocentric target position] ANOVA results on firing rates in target hold indicate that purely retinocentric encoding was rare: of 156 units with the effect of the final gaze, only 27 units showed a "purely retinocentric" effect in the separate two-way ANOVA, whereas most also showed the effect of initial gaze and/or the interaction. Third, only 25 of these 156 units showed an interaction between the initial gaze (i.e., saccade vector) and the final gaze in the two-way ANOVA on seven positions that were reached from more than one initial gaze position (cf. Fig. 4*B*). Fourth, an independent analysis that directly compared retinocentric vs. "screen-centered" (i.e., final gaze position dependent) reference frames confirmed that most units were classified as the latter in the target hold epoch, despite relying on only a small number of overlapping target locations for calculating screen-centered correlations. Hence, the most parsimonious explanation of our results suggests that eye position signals are indeed amply represented in the dorsal pulvinar.

It is important to note that the effects of initial vs. final gaze position were largely congruent (with a caveat of more extensive range for the final positions), and the influence of the

preceding memory saccade during the late part of the postsaccadic fixation was small. This implies that task epoch-specific aspects were not a major factor in gaze-dependent modulation. We did not explicitly test for potential influences of small corrective saccades (which occur before the start of the analyzed target hold epoch) or preparation of return saccades after the end of the trial, but we did not observe any systematic relationship between patterns of the final gaze position dependence and retinocentric visual/saccade tuning in the units that showed such tuning.

In respect to encoding of cue, delay, and saccade responses to the peripheral targets, our design allows dissociating between *1*) purely retinocentric encoding, *2*) retinocentric encoding modulated by gaze-dependent gain field, *3*) head/body/world-centered reference frame, and *4*) mixed reference frame. However, it is important to note that with the current design [largely nonoverlapping sets of final gaze positions linked to each of only 3 initial gaze positions, compared with, e.g., 9 starting positions in Andersen et al. (1990) or 9 horizontal targets in Mullette-Gillman et al. (2005)], if a unit shows not a "straightforward" gaze-specific gain effect on retinocentric encoding but a more complex pattern (e.g., shift or other idiosyncratic patterns), we cannot always reliably identify the best fitting reference frame (Mullette-Gillman et al. 2009). Future experiments with a larger range of initial and final target positions, and rotation of the head relative to the body and the body relative to the screen (Dean and Platt 2006), will elucidate the functional role of these signals in postural control and visually guided actions in space (Grieve et al. 2000).

Another potential limitation was that our experiments were not performed in total darkness, due to background illumination of the monitor. This could be considered as a potential confound because if a neuron has a large peripheral receptive field (RF), the initial (or final) gaze position might bring this RF outside of the illuminated monitor. This is, however, unlikely to explain our findings for several reasons. First, the horizontal size of the screen was large (84–91 degrees of visual angle). Second, a roughly equal number of units showed same or opposite hemifield preference for visual cue and initial gaze position. If the effects of gaze were due to changes in visual stimulation, we would expect these preferences to be opposite (regardless of whether a unit is showing enhancement or suppression to a bright cue) because a larger part of the illuminated screen is always in the hemifield opposite to the direction of the gaze. Third, many units did not have a clear visual response but still showed the effect of gaze position. Finally, the two studies that tested eye position effects in central thalamus and ventral pulvinar did not see a difference between light and darkness (Robinson et al. 1990; Schlag-Rey and Schlag 1984). To summarize, the eye position dependence during fixation is most likely due to extraretinal signals or nonretinocentric spatial encoding.

Functional Significance of Eye Position Signals in Dorsal Pulvinar

Generally, the functional significance of eye position signals in dPul is likely to be similar to that of other cortical and subcortical brain regions to which it connects, with the special property that the pulvinar is in a good anatomical position to distribute this information throughout the interconnected cortical circuitry (Saalmann and Kastner 2011; Sherman and Guillery 2002).

In respect to eye position dependence during fixation, the putative functions could include eye movements to auditory stimuli (Cohen and Andersen 2002; Yao and Peck 1997), computation of ocular vergence angle to determine depth/distance of foveated objects (Rosenbluth and Allman 2002), and maintaining stable fixation and smooth pursuit (Krauzlis et al. 2017; Ohtsuka et al. 1991). Because pulvinar neurons are binocular and are sensitive to relative retinal disparity, these cells may contribute to binocular depth perception (Casanova et al. 1991; Wilke et al. 2009). Indeed, pulvinar lesions in monkeys and humans can lead to stereoacuity deficits (Takayama et al. 1994), as well as gaze stabilization impairments such as nystagmus and impaired smooth pursuit (Ohtsuka et al. 1991; Wilke et al. 2010, 2018).

Previous electrophysiological and inactivation studies showed that the dorsal pulvinar is critical for guiding visuospatial attention (Fiebelkorn et al. 2019; Petersen et al. 1985). The fact that the preference for a certain steady gaze direction was also found in dPul neurons that do not have a visual cue response suggests that the eye position signals are not only used to further modulate peripheral visuospatial attention. Instead, the modulation of firing during steady fixation might represent attention to relevant spatial targets, encoded either foveally or in a nonretinocentric reference frame. Many dPul neurons decrease their firing during memory delay compared with that during initial fixation, suggesting that attention to peripheral locations and motor preparation might interact with foveal responses. Further work is required to dissociate these more cognitive possibilities from extraretinal orbital eye position signals.

There are multiple putative functions associated with influence of eye position on visual responses to peripheral targets and activity around saccades. Those include the transformation between retinal and egocentric limb/body coordinates (Andersen et al. 1993; Pouget and Snyder 2000), predictive shifts of visual attention associated with saccades (Duhamel et al. 1992; Hoffman and Subramaniam 1995; Wurtz et al. 2011b, 2011a), perceptual stability across eye movements (Mirpour and Bisley 2016; Sommer and Wurtz 2008), and recalibration of efference copy signals after a saccade (Wang et al. 2007; Xu et al. 2012).

Although the functional role of gaze dependence in dPul can be partly derived from related properties in connected cortical areas and the superior colliculus, it should be constrained by behavioral consequences of lesion and perturbation studies, as well as electrophysiological properties of dPul neurons. Given relatively coarse spatial tuning of most dPul responses to visual cues and saccades, and moderate effects of perturbation on saccadic precision and accuracy (Bender and Baizer 1990; Benevento and Port 1995; Dominguez-Vargas et al. 2017; Petersen et al. 1985; Robinson et al. 1986; Wilke et al. 2010), it is unlikely that the main function of eye position signals in dPul is precise perceptual or saccadic localization, as might be the case for SC and FEF (Caruso et al. 2018). The basic visuomotor characteristics of dPul seem to be closer to those of parietal areas LIP and 7a, as well as posterior cingulate (Andersen et al. 1990; Barash et al. 1991; Dean et al. 2004). There were, however, some differences between prevalent eye position effects in dPul and those cortical areas. For example, unlike in parietal cortex, the population-derived eye position

signal in the dPul was delayed relative to the saccade (Morris et al. 2012). In the premovement epochs, the encoding in dPul was mostly retinocentric or mixed, with a moderate occurrence of gaze-dependent gain fields. This is unlike more frequent gain fields in LIP (Andersen et al. 1990), the large number of neurons with nonretinocentric encoding that has been cautiously interpreted as head centered in parietal cortex (Caruso et al. 2018; Mullette-Gillman et al. 2005), or predominance of neurons exhibiting world-centered encoding in the posterior cingulate cortex (Dean and Platt 2006). Nonetheless, the diverse patterns of eye position dependence in dPul can support at least some aspects of spatial transformation from retinocentric encoding to other coordinate frames during visuomotor planning.

The transient effects of saccadic displacement from one stable eye position to another seem to be of less relevance in the dPul given that the number of units showing the effect of the current eye position on presaccadic and perisaccadic responses was small. Some dPul neurons increase their firing predictively during the memory delay and/or just before the saccade and are tuned to specific retinocentric locations, and might hypothetically participate in the transmission of the corollary discharge of the upcoming movement to the cortex, from the intermediate/deep layers of the superior colliculus or from one cortical area to another (Sherman and Guillery 2002; Wurtz et al. 2011b). More neurons, however, show pre/perisaccadic decrease of firing, consistent with a contribution to saccadic suppression (Wurtz et al. 2011b). The effect of the eye position on the immediate postsaccadic responses is stronger, and this epoch shows a mixture between retinocentric encoding of the preceding saccade vector (with or without modulation by the presaccadic eye position) and the encoding of the current (postsaccadic) eye position. Postsaccadic eye position-related gain fields have been shown to provide unreliable localization signal contaminated by the presaccadic eye position, and thus their functional role should be interpreted with caution (Xu et al. 2012).

Beyond the oculomotor scope of this study, there are strong indications that the dPul is important for visually guided reach and grasp movements (Acuña et al. 1990; Wilke et al. 2010, 2018), and likely eye-hand coordination (Grieve et al. 2000). In particular, the perturbation effects are not only space specific but also limb specific, with deficits stronger for the contralesional hand (Wilke et al. 2010, 2018), and dPul neurons respond differently when reaches are made with the left or the right hand (unpublished observations; see also Domínguez-Vargas 2017). In the context of reach and grasp movements, the integration of eye position is a crucial step in spatial transformations from retinocentric to trunk-, limb-, or world-centered reference frames (Batista et al. 2007; Battaglia-Mayer et al. 2003; Bosco et al. 2015; Boussaoud et al. 1998; Chang and Snyder 2010; Marzocchi et al. 2008; McGuire and Sabes 2011). In addition to limb movement aspects, gaze position has also been identified as an essential variable for stabilizing posture during upright standing (Ustinova and Perkins 2011). Although this variable has not been explicitly addressed in monkey research, we recently reported a patient with selective bilateral medial pulvinar lesions with difficulties in standing upright and walking, as well as nystagmus and hypometric saccades, without primary motor, vestibular, or sensory deficits (Wilke et al. 2017, 2018). It is thus conceivable that the dorsal pulvinar contribution to integration of postural signals goes beyond oculomotor and reach/grasp movements, a possibility that should be explored in neurophysiological experiments.

ACKNOWLEDGMENTS

We thank Ira Panolias, Daniela Lazzarini, Sina Plümer, Klaus Heisig, and Dirk Prüße for technical support. We also thank Stefan Treue, Alexander Gail, Hansjörg Scherberger, and members of the Decision and Awareness Group, Sensorimotor Group, and the Cognitive Neuroscience Laboratory for helpful discussions.

GRANTS

This work was supported by the Hermann and Lilly Schilling Foundation, German Research Foundation (DFG) Grants WI 4046/1-1 and Research Unit GA1475-B4, KA 3726/2-1, CNMPB Primate Platform, and funding from the Cognitive Neuroscience Laboratory.

DISCLOSURES

No conflicts of interest, financial or otherwise, are declared by the authors.

AUTHOR CONTRIBUTIONS

L.S., A.U.D.V., I.K., and M.W. conceived and designed research; A.U.D.V. and L.G. performed experiments; L.S., A.U.D.V., and L.G. analyzed data; L.S., A.U.D.V., L.G., I.K., and M.W. interpreted results of experiments; L.S. and I.K. prepared figures; L.S., I.K., and M.W. drafted manuscript; L.S., I.K., and M.W. edited and revised manuscript; L.S., I.K., and M.W. approved final version of manuscript.

REFERENCES

Acuña C, Cudeiro J, Gonzalez F, Alonso JM, Perez R. Lateral-posterior and pulvinar reaching cells–comparison with parietal area 5a: a study in behaving *Macaca nemestrina* monkeys. *Exp Brain Res* 82: 158–166, 1990. doi:10.1007/BF00230847.

Andersen RA, Bracewell RM, Barash S, Gnadt JW, Fogassi L. Eye position effects on visual, memory, and saccade-related activity in areas LIP and 7a of macaque. *J Neurosci* 10: 1176–1196, 1990. doi:10.1523/JNEUROSCI.10-04-01176.1990.

Andersen RA, Essick GK, Siegel RM. Encoding of spatial location by posterior parietal neurons. *Science* 230: 456–458, 1985. doi:10.1126/science.4048942.

Andersen RA, Mountcastle VB. The influence of the angle of gaze upon the excitability of the light-sensitive neurons of the posterior parietal cortex. *J Neurosci* 3: 532–548, 1983. doi:10.1523/JNEUROSCI.03-03-00532.1983.

Andersen RA, Snyder LH, Li CS, Stricanne B. Coordinate transformations in the representation of spatial information. *Curr Opin Neurobiol* 3: 171–176, 1993. doi:10.1016/0959-4388(93)90206-E.

Arcaro MJ, Pinsk MA, Chen J, Kastner S. Organizing principles of pulvino-cortical functional coupling in humans. *Nat Commun* 9: 5382, 2018. [Erratum in *Nat Commun* 10: 1443, 2019.] doi:10.1038/s41467-018-07725-6.

Arend I, Machado L, Ward R, McGrath M, Ro T, Rafal RD. The role of the human pulvinar in visual attention and action: evidence from temporal-order judgment, saccade decision, and antisaccade tasks. *Prog Brain Res* 171: 475–483, 2008. doi:10.1016/S0079-6123(08)00669-9.

Bakker R, Tiesinga P, Kötter R. The Scalable Brain Atlas: instant web-based access to public brain atlases and related content. *Neuroinformatics* 13: 353–366, 2015. doi:10.1007/s12021-014-9258-x.

Baldwin MK, Bourne JA. The evolution of subcortical pathways to the extrastriate cortex (2nd ed.). In: *Evolution of Nervous Systems*, edited by Kaas JH. Oxford, UK: Academic, 2017, p. 165–185.

Barash S, Bracewell RM, Fogassi L, Gnadt JW, Andersen RA. Saccade-related activity in the lateral intraparietal area. II. Spatial properties. *J Neurophysiol* 66: 1109–1124, 1991. doi:10.1152/jn.1991.66.3.1109.

Barton EJ, Sparks DL. Saccades to remembered targets exhibit enhanced orbital position effects in monkeys. *Vision Res* 41: 2393–2406, 2001. doi:10.1016/S0042-6989(01)00130-4.

Batista AP, Santhanam G, Yu BM, Ryu SI, Afshar A, Shenoy KV. Reference frames for reach planning in macaque dorsal premotor cortex. *J Neurophysiol* 98: 966–983, 2007. doi:10.1152/jn.00421.2006.

Battaglia-Mayer A, Caminiti R, Lacquaniti F, Zago M. Multiple levels of representation of reaching in the parieto-frontal network. *Cereb Cortex* 13: 1009–1022, 2003. doi:10.1093/cercor/13.10.1009.

Bender DB. Visual activation of neurons in the primate pulvinar depends on cortex but not colliculus. *Brain Res* 279: 258–261, 1983. doi:10.1016/0006-8993(83)90188-9.

Bender DB, Baizer JS. Saccadic eye movements following kainic acid lesions of the pulvinar in monkeys. *Exp Brain Res* 79: 467–478, 1990. doi:10.1007/BF00229317.

Bender DB, Butter CM. Comparison of the effects of superior colliculus and pulvinar lesions on visual search and tachistoscopic pattern discrimination in monkeys. *Exp Brain Res* 69: 140–154, 1987. doi:10.1007/BF00247037.

Benevento LA, Port JD. Single neurons with both form/color differential responses and saccade-related responses in the nonretinotopic pulvinar of the behaving macaque monkey. *Vis Neurosci* 12: 523–544, 1995. doi:10.1017/S0952523800008439.

Benevento LA, Standage GP. The organization of projections of the retinorecipient and nonretinorecipient nuclei of the pretectal complex and layers of the superior colliculus to the lateral pulvinar and medial pulvinar in the macaque monkey. *J Comp Neurol* 217: 307–336, 1983. doi:10.1002/cne.902170307.

Berman RA, Wurtz RH. Signals conveyed in the pulvinar pathway from superior colliculus to cortical area MT. *J Neurosci* 31: 373–384, 2011. doi:10.1523/JNEUROSCI.4738-10.2011.

Bickford ME. Thalamic circuit diversity: modulation of the driver/modulator framework. *Front Neural Circuits* 9: 86, 2016. doi:10.3389/fncir.2015.00086.

Bizzi E. Discharge of frontal eye field neurons during saccadic and following eye movements in unanesthetized monkeys. *Exp Brain Res* 6: 69–80, 1968. doi:10.1007/BF00235447.

Bosco A, Breveglieri R, Reser D, Galletti C, Fattori P. Multiple representation of reaching space in the medial posterior parietal area V6A. *Cereb Cortex* 25: 1654–1667, 2015. doi:10.1093/cercor/bht420.

Boussaoud D, Jouffrais C, Bremmer F. Eye position effects on the neuronal activity of dorsal premotor cortex in the macaque monkey. *J Neurophysiol* 80: 1132–1150, 1998. doi:10.1152/jn.1998.80.3.1132.

Brainard DH. The psychophysics toolbox. *Spat Vis* 10: 433–436, 1997. doi:10.1163/156856897X00357.

Bremmer F. Eye position effects in macaque area V4. *Neuroreport* 11: 1277–1283, 2000. doi:10.1097/00001756-200004270-00027.

Bremmer F, Distler C, Hoffmann KP. Eye position effects in monkey cortex. II. Pursuit- and fixation-related activity in posterior parietal areas LIP and 7A. *J Neurophysiol* 77: 962–977, 1997. doi:10.1152/jn.1997.77.2.962.

Bremmer F, Duhamel JR, Ben Hamed S, Graf W. Heading encoding in the macaque ventral intraparietal area (VIP). *Eur J Neurosci* 16: 1554–1568, 2002. doi:10.1046/j.1460-9568.2002.02207.x.

Bremmer F, Graf W, Ben Hamed S, Duhamel JR. Eye position encoding in the macaque ventral intraparietal area (VIP). *Neuroreport* 10: 873–878, 1999. doi:10.1097/00001756-199903170-00037.

Bremmer F, Pouget A, Hoffmann KP. Eye position encoding in the macaque posterior parietal cortex. *Eur J Neurosci* 10: 153–160, 1998. doi:10.1046/j.1460-9568.1998.00010.x.

Bridge H, Leopold DA, Bourne JA. Adaptive pulvinar circuitry supports visual cognition. *Trends Cogn Sci* 20: 146–157, 2016. doi:10.1016/j.tics.2015.10.003.

Brotchie PR, Andersen RA, Snyder LH, Goodman SJ. Head position signals used by parietal neurons to encode locations of visual stimuli. *Nature* 375: 232–235, 1995. doi:10.1038/375232a0.

Campos M, Cherian A, Segraves MA. Effects of eye position upon activity of neurons in macaque superior colliculus. *J Neurophysiol* 95: 505–526, 2006. doi:10.1152/jn.00639.2005.

Cappe C, Morel A, Barone P, Rouiller EM. The thalamocortical projection systems in primate: an anatomical support for multisensory and sensorimotor interplay. *Cereb Cortex* 19: 2025–2037, 2009. doi:10.1093/cercor/bhn228.

Cappe C, Morel A, Rouiller EM. Thalamocortical and the dual pattern of corticothalamic projections of the posterior parietal cortex in macaque monkeys. *Neuroscience* 146: 1371–1387, 2007. doi:10.1016/j.neuroscience.2007.02.033.

Cappe C, Rouiller EM, Barone P. Cortical and thalamic pathways for multisensory and sensorimotor interplay. In: *The Neural Bases of Multisensory Processes*, edited by Murray MM, Wallace MT. Boca Raton, FL: CRC/Taylor & Francis, 2012.

Caruso VC, Pages DS, Sommer MA, Groh JM. Beyond the labeled line: variation in visual reference frames from intraparietal cortex to frontal eye fields and the superior colliculus. *J Neurophysiol* 119: 1411–1421, 2018. doi:10.1152/jn.00584.2017.

Casanova C, Molotchnikoff S. Influence of the superior colliculus on visual responses of cells in the rabbit's lateral posterior nucleus. *Exp Brain Res* 80: 387–396, 1990. doi:10.1007/BF00228166.

Casanova C, Nordmann JP, Molotchnikoff S. [Pulvina-lateralis posterior nucleus complex of mammals and the visual function]. *J Physiol (Paris)* 85: 44–57, 1991.

Chang SW, Snyder LH. Idiosyncratic and systematic aspects of spatial representations in the macaque parietal cortex. *Proc Natl Acad Sci USA* 107: 7951–7956, 2010. doi:10.1073/pnas.0913209107.

Cohen YE, Andersen RA. A common reference frame for movement plans in the posterior parietal cortex. *Nat Rev Neurosci* 3: 553–562, 2002. doi:10.1038/nrn873.

Colby CL. Action-oriented spatial reference frames in cortex. *Neuron* 20: 15–24, 1998. doi:10.1016/S0896-6273(00)80429-8.

Crapse TB, Sommer MA. Corollary discharge circuits in the primate brain. *Curr Opin Neurobiol* 18: 552–557, 2008. doi:10.1016/j.conb.2008.09.017.

Cudeiro J, González F, Pérez R, Alonso JM, Acuña C. Does the pulvinar-LP complex contribute to motor programming? *Brain Res* 484: 367–370, 1989. doi:10.1016/0006-8993(89)90383-1.

Dean HL, Crowley JC, Platt ML. Visual and saccade-related activity in macaque posterior cingulate cortex. *J Neurophysiol* 92: 3056–3068, 2004. doi:10.1152/jn.00691.2003.

Dean HL, Platt ML. Allocentric spatial referencing of neuronal activity in macaque posterior cingulate cortex. *J Neurosci* 26: 1117–1127, 2006. doi:10.1523/JNEUROSCI.2497-05.2006.

Domínguez-Vargas AU. *The Role of Thalamic Pulvinar in Eye-Hand Coordination for Goal-Directed Actions* (PhD thesis). Göttingen, Germany: Georg-August-Universität Göttingen, 2017.

Dominguez-Vargas AU, Schneider L, Wilke M, Kagan I. Electrical microstimulation of the pulvinar biases saccade choices and reaction times in a time-dependent manner. *J Neurosci* 37: 2234–2257, 2017. doi:10.1523/JNEUROSCI.1984-16.2016.

Duhamel JR, Colby CL, Goldberg ME. The updating of the representation of visual space in parietal cortex by intended eye movements. *Science* 255: 90–92, 1992. doi:10.1126/science.1553535.

Durand J-B, Trotter Y, Celebrini S. Privileged processing of the straight-ahead direction in primate area V1. *Neuron* 66: 126–137, 2010. doi:10.1016/j.neuron.2010.03.014.

Fiebelkorn IC, Pinsk MA, Kastner S. The mediodorsal pulvinar coordinates the macaque fronto-parietal network during rhythmic spatial attention. *Nat Commun* 10: 215, 2019. doi:10.1038/s41467-018-08151-4.

Galletti C, Battaglini PP, Fattori P. Eye position influence on the parieto-occipital area PO (V6) of the macaque monkey. *Eur J Neurosci* 7: 2486–2501, 1995. doi:10.1111/j.1460-9568.1995.tb01047.x.

Genovesio A, Brunamonti E, Giusti MA, Ferraina S. Postsaccadic activities in the posterior parietal cortex of primates are influenced by both eye movement vectors and eye position. *J Neurosci* 27: 3268–3273, 2007. doi:10.1523/JNEUROSCI.5415-06.2007.

Grieve KL, Acuña C, Cudeiro J. The primate pulvinar nuclei: vision and action. *Trends Neurosci* 23: 35–39, 2000. doi:10.1016/S0166-2236(99)01482-4.

Guthrie BL, Porter JD, Sparks DL. Corollary discharge provides accurate eye position information to the oculomotor system. *Science* 221: 1193–1195, 1983. doi:10.1126/science.6612334.

Gutierrez C, Cola MG, Seltzer B, Cusick C. Neurochemical and connectional organization of the dorsal pulvinar complex in monkeys. *J Comp Neurol* 419: 61–86, 2000. doi:10.1002/(SICI)1096-9861(20000327)419:1<61:AID-CNE4>3.0.CO;2-I.

Halassa MM, Kastner S. Thalamic functions in distributed cognitive control. *Nat Neurosci* 20: 1669–1679, 2017. doi:10.1038/s41593-017-0020-1.

Harting JK, Huerta MF, Frankfurter AJ, Strominger NL, Royce GJ. Ascending pathways from the monkey superior colliculus: an autoradiographic analysis. *J Comp Neurol* 192: 853–882, 1980. doi:10.1002/cne.901920414.

Hernández RG, Calvo PM, Blumer R, de la Cruz RR, Pastor AM. Functional diversity of motoneurons in the oculomotor system. *Proc Natl Acad Sci USA* 116: 3837–3846, 2019. doi:10.1073/pnas.1818524116.

Hoffman JE, Subramaniam B. The role of visual attention in saccadic eye movements. *Percept Psychophys* 57: 787–795, 1995. doi:10.3758/BF03206794.

Itoh K, Mizuno N. A cerebello-pulvinar projection in the cat as visualized by the use of anterograde transport of horseradish peroxidase. *Brain Res* 171: 131–134, 1979. doi:10.1016/0006-8993(79)90738-8.

Jones EG. The lateral posterior and pulvinar nuclei. In: *The Thalamus*. Cambridge, UK: Cambridge University Press, 2007, p. 1009–1071.

Kaas JH, Lyon DC. Pulvinar contributions to the dorsal and ventral streams of visual processing in primates. *Brain Res Brain Res Rev* 55: 285–296, 2007. doi:10.1016/j.brainresrev.2007.02.008.

Karnath HO, Himmelbach M, Rorden C. The subcortical anatomy of human spatial neglect: putamen, caudate nucleus and pulvinar. *Brain* 125: 350–360, 2002. doi:10.1093/brain/awf032.

Kinoshita M, Kato R, Isa K, Kobayashi K, Kobayashi K, Onoe H, Isa T. Dissecting the circuit for blindsight to reveal the critical role of pulvinar and superior colliculus. *Nat Commun* 10: 135, 2019. doi:10.1038/s41467-018-08058-0.

Krauzlis RJ, Goffart L, Hafed ZM. Neuronal control of fixation and fixational eye movements. *Philos Trans R Soc Lond B Biol Sci* 372: 20160205, 2017. doi:10.1098/rstb.2016.0205.

Lal R, Friedlander MJ. Gating of retinal transmission by afferent eye position and movement signals. *Science* 243: 93–96, 1989. doi:10.1126/science.2911723.

Lehky SR, Sereno ME, Sereno AB. Characteristics of eye-position gain field populations determine geometry of visual space. *Front Integr Neurosci* 9: 72, 2016. doi:10.3389/fnint.2015.00072.

Luschei ES, Fuchs AF. Activity of brain stem neurons during eye movements of alert monkeys. *J Neurophysiol* 35: 445–461, 1972. doi:10.1152/jn.1972.35.4.445.

Marzocchi N, Breveglieri R, Galletti C, Fattori P. Reaching activity in parietal area V6A of macaque: eye influence on arm activity or retinocentric coding of reaching movements? *Eur J Neurosci* 27: 775–789, 2008. doi:10.1111/j.1460-9568.2008.06021.x.

McGuire LM, Sabes PN. Heterogeneous representations in the superior parietal lobule are common across reaches to visual and proprioceptive targets. *J Neurosci* 31: 6661–6673, 2011. doi:10.1523/JNEUROSCI.2921-10.2011.

Mirpour K, Bisley JW. Remapping, spatial stability, and temporal continuity: from the pre-saccadic to postsaccadic representation of visual space in LIP. *Cereb Cortex* 26: 3183–3195, 2016. doi:10.1093/cercor/bhv153.

Morris AP, Bremmer F, Krekelberg B. Eye-position signals in the dorsal visual system are accurate and precise on short timescales. *J Neurosci* 33: 12395–12406, 2013. doi:10.1523/JNEUROSCI.0576-13.2013.

Morris AP, Krekelberg B. A stable visual world in primate primary visual cortex. *Curr Biol* 29: 1471–1480.e6, 2019. doi:10.1016/j.cub.2019.03.069.

Morris AP, Kubischik M, Hoffmann KP, Krekelberg B, Bremmer F. Dynamics of eye-position signals in the dorsal visual system. *Curr Biol* 22: 173–179, 2012. doi:10.1016/j.cub.2011.12.032.

Mullette-Gillman OA, Cohen YE, Groh JM. Eye-centered, head-centered, and complex coding of visual and auditory targets in the intraparietal sulcus. *J Neurophysiol* 94: 2331–2352, 2005. doi:10.1152/jn.00021.2005.

Mullette-Gillman OA, Cohen YE, Groh JM. Motor-related signals in the intraparietal cortex encode locations in a hybrid, rather than eye-centered reference frame. *Cereb Cortex* 19: 1761–1775, 2009. doi:10.1093/cercor/bhn207.

Noda H, Warabi T. Eye position signals in the flocculus of the monkey during smooth-pursuit eye movements. *J Physiol* 324: 187–202, 1982. doi:10.1113/jphysiol.1982.sp014106.

Ohayon S, Tsao DY. MR-guided stereotactic navigation. *J Neurosci Methods* 204: 389–397, 2012. doi:10.1016/j.jneumeth.2011.11.031.

Ohtsuka K, Igarashi Y, Maekawa H, Nakagawa T. Pursuit deficits in bilateral pulvinar lesions. *Ophthalmologica* 203: 196–202, 1991. doi:10.1159/000310252.

Padberg J, Cerkevich C, Engle J, Rajan AT, Recanzone G, Kaas J, Krubitzer L. Thalamocortical connections of parietal somatosensory cortical fields in macaque monkeys are highly divergent and convergent. *Cereb Cortex* 19: 2038–2064, 2009. doi:10.1093/cercor/bhn229.

Patel VR, Zee DS. The cerebellum in eye movement control: nystagmus, coordinate frames and disconjugacy. *Eye (Lond)* 29: 191–195, 2015. [Erratum in *Eye (Lond)* 29: 299, 2015.] doi:10.1038/eye.2014.271.

Peck CK, Schlag-Rey M, Schlag J. Visuo-oculomotor properties of cells in the superior colliculus of the alert cat. *J Comp Neurol* 194: 97–116, 1980. doi:10.1002/cne.901940106.

Petersen SE, Robinson DL, Keys W. Pulvinar nuclei of the behaving rhesus monkey: visual responses and their modulation. *J Neurophysiol* 54: 867–886, 1985. doi:10.1152/jn.1985.54.4.867.

Petersen SE, Robinson DL, Morris JD. Contributions of the pulvinar to visual spatial attention. *Neuropsychologia* 25: 97–105, 1987. doi:10.1016/0028-3932(87)90046-7.

Porter KK, Metzger RR, Groh JM. Representation of eye position in primate inferior colliculus. *J Neurophysiol* 95: 1826–1842, 2006. doi:10.1152/jn.00857.2005.

Pouget A, Sejnowski TJ. Spatial transformations in the parietal cortex using basis functions. *J Cogn Neurosci* 9: 222–237, 1997. doi:10.1162/jocn.1997.9.2.222.

Pouget A, Snyder LH. Computational approaches to sensorimotor transformations. *Nat Neurosci* 3, *Suppl*: 1192–1198, 2000. doi:10.1038/81469.

Preuss TM. Evolutionary specializations of primate brain systems. In: *Primate Origins: Evolution and Adaptations*, edited by Ravosa MJ, Dagosto M. New York: Springer, 2007, p. 625–675.

Przybyszewski AW, Kagan I, Snodderly DM. Primate area V1: largest response gain for receptive fields in the straight-ahead direction. *Neuroreport* 25: 1109–1115, 2014. doi:10.1097/WNR.0000000000000235.

Robinson DL. Functional contributions of the primate pulvinar. *Prog Brain Res* 95: 371–380, 1993. doi:10.1016/S0079-6123(08)60382-9.

Robinson DL, McClurkin JW, Kertzman C. Orbital position and eye movement influences on visual responses in the pulvinar nuclei of the behaving macaque. *Exp Brain Res* 82: 235–246, 1990. doi:10.1007/BF00231243.

Robinson DL, Petersen SE. The pulvinar and visual salience. *Trends Neurosci* 15: 127–132, 1992. doi:10.1016/0166-2236(92)90354-B.

Robinson DL, Petersen SE, Keys W. Saccade-related and visual activities in the pulvinar nuclei of the behaving rhesus monkey. *Exp Brain Res* 62: 625–634, 1986. doi:10.1007/BF00236042.

Rodrigo-Angulo ML, Reinoso-Suarez F. Cerebellar projections to the lateral posterior-pulvinar thalamic complex in the cat. *Brain Res* 322: 172–176, 1984. doi:10.1016/0006-8993(84)91200-9.

Rohlfing T, Kroenke CD, Sullivan EV, Dubach MF, Bowden DM, Grant KA, Pfefferbaum A. The INIA19 template and NeuroMaps atlas for primate brain image parcellation and spatial normalization. *Front Neuroinform* 6: 27, 2012. doi:10.3389/fninf.2012.00027.

Romanski LM, Giguere M, Bates JF, Goldman-Rakic PS. Topographic organization of medial pulvinar connections with the prefrontal cortex in the rhesus monkey. *J Comp Neurol* 379: 313–332, 1997. doi:10.1002/(SICI)1096-9861(19970317)379:3<313:AID-CNE1>3.0.CO;2-6.

Rosenbluth D, Allman JM. The effect of gaze angle and fixation distance on the responses of neurons in V1, V2, and V4. *Neuron* 33: 143–149, 2002. doi:10.1016/S0896-6273(01)00559-1.

Rovó Z, Ulbert I, Acsády L. Drivers of the primate thalamus. *J Neurosci* 32: 17894–17908, 2012. doi:10.1523/JNEUROSCI.2815-12.2012.

Saalmann YB, Kastner S. Cognitive and perceptual functions of the visual thalamus. *Neuron* 71: 209–223, 2011. doi:10.1016/j.neuron.2011.06.027.

Sajad A, Sadeh M, Yan X, Wang H, Crawford JD. Transition from target to gaze coding in primate frontal eye field during memory delay and memory–motor transformation. *eNeuro* 3: ENEURO.0040-16.2016, 2016. doi:10.1523/ENEURO.0040-16.2016.

Sakata H, Shibutani H, Kawano K. Spatial properties of visual fixation neurons in posterior parietal association cortex of the monkey. *J Neurophysiol* 43: 1654–1672, 1980. doi:10.1152/jn.1980.43.6.1654.

Salinas E, Abbott LF. Coordinate transformation in the visual system: how to generate gain fields and what to compute with them. In: *Advances in Neural Population Coding*, edited by Nicolelis MA. Elsevier, 2001, vol. 130, p. 175–190.

Schlag J, Schlag-Rey M, Peck CK, Joseph JP. Visual responses of thalamic neurons depending on the direction of gaze and the position of targets in space. *Exp Brain Res* 40: 170–184, 1980. doi:10.1007/BF00237535.

Schlag-Rey M, Schlag J. Visuomotor functions of central thalamus in monkey. I. Unit activity related to spontaneous eye movements. *J Neurophysiol* 51: 1149–1174, 1984. doi:10.1152/jn.1984.51.6.1149.

Schmahmann JD, Pandya DN. Anatomical investigation of projections from thalamus to posterior parietal cortex in the rhesus monkey: a WGA-HRP and fluorescent tracer study. *J Comp Neurol* 295: 299–326, 1990. doi:10.1002/cne.902950212.

Schmidt M, Sudkamp S, Wahle P. Characterization of pretectal-nuclear-complex afferents to the pulvinar in the cat. *Exp Brain Res* 138: 509–519, 2001. doi:10.1007/s002210100738.

Schmitt LI, Wimmer RD, Nakajima M, Happ M, Mofakham S, Halassa MM. Thalamic amplification of cortical connectivity sustains attentional control. *Nature* 545: 219–223, 2017. doi:10.1038/nature22073.

Sherman SM, Guillery RW. The role of the thalamus in the flow of information to the cortex. *Philos Trans R Soc Lond B Biol Sci* 357: 1695–1708, 2002. doi:10.1098/rstb.2002.1161.

Sommer MA, Wurtz RH. Visual perception and corollary discharge. *Perception* 37: 408–418, 2008. doi:10.1068/p5873.

Squatrito S, Maioli MG. Gaze field properties of eye position neurones in areas MST and 7a of the macaque monkey. *Vis Neurosci* 13: 385–398, 1996. doi:10.1017/S0952523800007628.

Sudkamp S, Schmidt M. Response characteristics of neurons in the pulvinar of awake cats to saccades and to visual stimulation. *Exp Brain Res* 133: 209–218, 2000. doi:10.1007/s002210000374.

Sultan F, Augath M, Hamodeh S, Murayama Y, Oeltermann A, Rauch A, Thier P. Unravelling cerebellar pathways with high temporal precision targeting motor and extensive sensory and parietal networks. *Nat Commun* 3: 924, 2012. doi:10.1038/ncomms1912.

Sylvestre PA, Cullen KE. Quantitative analysis of abducens neuron discharge dynamics during saccadic and slow eye movements. *J Neurophysiol* 82: 2612–2632, 1999. doi:10.1152/jn.1999.82.5.2612.

Takayama Y, Sugishita M, Kido T, Ogawa M, Fukuyama H, Akiguchi I. Impaired stereoacuity due to a lesion in the left pulvinar. *J Neurol Neurosurg Psychiatry* 57: 652–654, 1994. doi:10.1136/jnnp.57.5.652.

Tanaka M. Spatiotemporal properties of eye position signals in the primate central thalamus. *Cereb Cortex* 17: 1504–1515, 2007. doi:10.1093/cercor/bhl061.

Tanaka M, Kunimatsu J. Contribution of the central thalamus to the generation of volitional saccades. *Eur J Neurosci* 33: 2046–2057, 2011. doi:10.1111/j.1460-9568.2011.07699.x.

Trotter Y, Celebrini S. Gaze direction controls response gain in primary visual-cortex neurons. *Nature* 398: 239–242, 1999. doi:10.1038/18444.

Ustinova K, Perkins J. Gaze and viewing angle influence visual stabilization of upright posture. *Brain Behav* 1: 19–25, 2011. doi:10.1002/brb3.10.

Van der Stigchel S, Arend I, van Koningsbruggen MG, Rafal RD. Oculomotor integration in patients with a pulvinar lesion. *Neuropsychologia* 48: 3497–3504, 2010. doi:10.1016/j.neuropsychologia.2010.07.035.

Van Opstal AJ, Hepp K, Suzuki Y, Henn V. Influence of eye position on activity in monkey superior colliculus. *J Neurophysiol* 74: 1593–1610, 1995. doi:10.1152/jn.1995.74.4.1593.

Wang X, Zhang M, Cohen IS, Goldberg ME. The proprioceptive representation of eye position in monkey primary somatosensory cortex. *Nat Neurosci* 10: 640–646, 2007. doi:10.1038/nn1878.

Wilke M, Dechent P, Bähr M. Sarcoidosis manifestion centered on the thalamic pulvinar leading to persistent astasia. *Mov Disord Clin Pract (Hoboken)* 4: 898–900, 2017. doi:10.1002/mdc3.12544.

Wilke M, Kagan I, Andersen RA. Effects of pulvinar inactivation on spatial decision-making between equal and asymmetric reward options. *J Cogn Neurosci* 25: 1270–1283, 2013. doi:10.1162/jocn_a_00399.

Wilke M, Mueller KM, Leopold DA. Neural activity in the visual thalamus reflects perceptual suppression. *Proc Natl Acad Sci USA* 106: 9465–9470, 2009. doi:10.1073/pnas.0900714106.

Wilke M, Schneider L, Dominguez-Vargas AU, Schmidt-Samoa C, Milosserdov K, Nazzal A, Dechent P, Cabral-Calderin Y, Scherberger H, Kagan I, Bähr M. Reach and grasp deficits following damage to the dorsal pulvinar. *Cortex* 99: 135–149, 2018. doi:10.1016/j.cortex.2017.10.011.

Wilke M, Turchi J, Smith K, Mishkin M, Leopold DA. Pulvinar inactivation disrupts selection of movement plans. *J Neurosci* 30: 8650–8659, 2010. doi:10.1523/JNEUROSCI.0953-10.2010.

Wurtz RH, Joiner WM, Berman RA. Neuronal mechanisms for visual stability: progress and problems. *Philos Trans R Soc Lond B Biol Sci* 366: 492–503, 2011a. doi:10.1098/rstb.2010.0186.

Wurtz RH, McAlonan K, Cavanaugh J, Berman RA. Thalamic pathways for active vision. *Trends Cogn Sci* 15: 177–184, 2011b. doi:10.1016/j.tics.2011.02.004.

Wurtz RH, Sommer MA, Cavanaugh J. Drivers from the deep: the contribution of collicular input to thalamocortical processing. *Prog Brain Res* 149: 207–225, 2005. doi:10.1016/S0079-6123(05)49015-9.

Wyder MT, Massoglia DP, Stanford TR. Quantitative assessment of the timing and tuning of visual-related, saccade-related, and delay period activity in primate central thalamus. *J Neurophysiol* 90: 2029–2052, 2003. doi:10.1152/jn.00064.2003.

Xu BY, Karachi C, Goldberg ME. The postsaccadic unreliability of gain fields renders it unlikely that the motor system can use them to calculate target position in space. *Neuron* 76: 1201–1209, 2012. doi:10.1016/j.neuron.2012.10.034.

Xu Y, Wang X, Peck C, Goldberg ME. The time course of the tonic oculomotor proprioceptive signal in area 3a of somatosensory cortex. *J Neurophysiol* 106: 71–77, 2011. doi:10.1152/jn.00668.2010.

Yao L, Peck CK. Saccadic eye movements to visual and auditory targets. *Exp Brain Res* 115: 25–34, 1997. doi:10.1007/PL00005682.

Yeterian EH, Pandya DN. Thalamic connections of the cortex of the superior temporal sulcus in the rhesus monkey. *J Comp Neurol* 282: 80–97, 1989. doi:10.1002/cne.902820107.

Zhou NA, Maire PS, Masterson SP, Bickford ME. The mouse pulvinar nucleus: Organization of the tectorecipient zones. *Vis Neurosci* 34: E011, 2017. doi:10.1017/S0952523817000050.

Ziesche A, Hamker FH. A computational model for the influence of corollary discharge and proprioception on the perisaccadic mislocalization of briefly presented stimuli in complete darkness. *J Neurosci* 31: 17392–17405, 2011. doi:10.1523/JNEUROSCI.3407-11.2011.

Zipser D, Andersen RA. A back-propagation programmed network that simulates response properties of a subset of posterior parietal neurons. *Nature* 331: 679–684, 1988. doi:10.1038/331679a0.